Ana Isabel Gomes da Mata

PDT-GENERATED ANTITUMOUR VACCINES

Master in Medicinal Chemistry
Chemistry Department
FCTUC

September, 2015

· U C ·

Universidade de Coimbra

Ana Isabel Gomes da Mata

PDT-GENERATED ANTITUMOUR VACCINES

Dissertation submitted for the degree of Master in Medicinal Chemistry

Professor Luis G. Arnaut

Lígia C. Gomes-da-Silva

September 2015

University of Coimbra

« The most beautiful experience we can have is the mysterious – the fundamental emotion which stands at the cradle of true art and true science. »

Albert Einstein

Para a minha irmã, Carla Mata

AGRADECIMENTOS

No final de mais uma etapa, não me posso esquecer de todos os que me acompanharam na viagem e tornaram possível esta realidade. Por isso, quero agradecer:

Ao meu orientador Prof. Doutor Luis Arnaut, pelo seu apoio científico e incentivo que forneceu ao longo deste projecto. O constante estímulo e orientação construtiva concedidos durante este ano foram indispensáveis para fomentar o meu crescimento pessoal e académico.

À minha co-orientadora, Doutora Lígia Gomes-da-Silva, pela sua amizade, disponibilidade, acompanhamento e ajuda em todas as dificuldades. Com a sua energia e simpatia contagiantes, o seu apoio incondicional e interesse no decorrer deste estudo fez com que nunca deixasse de estar "presente" no quotidiano do nosso grupo.

A todo o grupo de Estrutura, Energia e Reactividade, que me acolheu e foi uma companhia constante que sempre fomentou a discussão e troca de ideias entre os diferentes elementos, com o propósito de expandirmos os nossos horizontes ao nos envolvermos nos diferentes projectos em curso e ajudarmo-nos mutuamente. Ao Mestre Hélder Soares, que foi uma fonte de ajuda incansável na colaboração neste trabalho. Ao Doutor Fábio Schaberle, pelo acompanhamento e estímulo na procura de saber mais para além do requerido, assim como na assistência de utilização do laser de picossegundos para este projecto. À Mestre Kamila Mentel, pela orientação e companhia que ainda me proporciona desde o início, assim como pelo seu carácter efusivo que é sempre capaz de me alegrar. A todos vós, pela vossa amizade.

À Luzitin, SA, por fornecer a redaporfin.

Ao Prof. Doutor José Paixão do grupo de Estrutura Electrónica e Magnéticas dos Materiais, no Departamento de Física, pela ajuda na utilização do gerador de raios-X.

Aos meus amigos e colegas de laboratório Ana Catarina Lobo, Alexandre Silva e Joana Campos, que me acompanharam neste ano, por tudo o que passámos juntos, desde a companhia durante as longas experiências no laboratório, às partilhas de experiências nos congressos (e *coffee-breaks*). Obrigada também pela vossa amizade, pelos momentos de descontracção, pela vossa preocupação e apoio incondicional.

A todos os colegas de Mestrado pela vossa camaradagem e amizade. À Carolina Vinagreiro, à Vanessa Tomé e à Ana Rita Ferreira, um agradecimento especial por terem sido uma presença constante, com quem pude partilhar grande parte do meu percurso académico, sabendo que podia contar com a vossa ajuda para tudo o que fosse preciso.

Aos meus amigos pelo carinho e compreensão. À Francisca Oliveira, à Jéssica Reis e à Ana Bárbara, por todas as vezes que me convidaram a sair e a esquecer o *stress* por umas horas, por todas as conversas intermináveis em que partilhámos preocupações, opiniões, ideias, projectos e sonhos. A vossa amizade vale muito mais do que possam imaginar. Obrigada por me ajudarem a encontrar o equilíbrio: sem vocês, não teria conseguido chegar até aqui. Desculpem-me todos os momentos que não pude passar convosco.

À minha família, por todas as oportunidades que me concederam, pelo apoio e confiança nas minhas decisões e pelo amor e orgulho que demostraram. Aos meus pais e avós, pela compreensão e incentivo dados ao longo destes anos, pelo esforço em se ajustarem aos meus horários inconstantes de modo a ajudarem como pudessem e por toda a sua dedicação a mim e à minha irmã. À minha tia, por ser um apoio indispensável, pela sabedoria e paciência demonstradas sempre que precisava da sua ajuda, pelo seu entusiasmo e interesse no meu trabalho e por tudo o que faz para que possa tirar o melhor proveito da vida académica. À minha irmã, pela "infindável" paciência de me ouvir falar dos mais diversos assuntos e dar-me conselhos ou sugestões, pela sua preocupação em saber sempre como corriam as coisas, por todas as vezes que me fez sorrir para me distrair de quaisquer inquietações que tivesse e, no fundo, por ser quem é: a pessoa mais importante na minha vida. Obrigada por tudo.

PDT-Generated Antitumour Vaccines

Ana I.G. Mata*, Lígia C.Gomes-da-Silva, Hélder T. Soares, and Luis G. Arnaut

Chemistry Department, University of Coimbra, Largo Paço do Conde, 3004-531 Coimbra, Portugal

Received September 3rd, 2015 (Revised September 9th, 2015)

KEYWORDS: antitumour vaccines; cancer; immunogenic cell death; prophylactic vaccines; photodynamic therapy; redaporfin; 4T1 cell line; CT26 cell line

ABSTRACT: Photodynamic therapy (PDT) is an established clinical treatment modality for cancer and other non-malignant diseases, requiring the combined use of a photosensitizer (PS), light irradiation of a specific wavelength for each PS, and oxygen to generate reactive oxygen species (ROS) responsible for destroying the tumour. We use *in vitro* PDT with the photosensitizer (PS) redaporfin to generate prophylactic whole-cell antitumour vaccines and evaluate the immunogenicity of two optimization protocols. In the first protocol, 4T1 cells were incubated with the PS, underwent different doses of PDT to modulate apoptotic/necrotic cell death. After a 24 h post-PDT incubation, the cells were irradiated with picosecond UV to generate the vaccine. Different treatment groups (Apoptosis/UV; Necrosis/UV; UV control) of BALB/c mice were subcutaneously vaccinated with 3.00 x 10^6 treated cells. After a week, they were subcutaneously inoculated with 350,000 viable cells for the tumour challenge. The results did not have statistical significance nor showed immunogenic effect between the treatment groups and the negative control. In the subsequent protocol, we changed to the CT26 cell line, and the post-PDT incubation time was shortened to 4 h without UV picosecond irradiation. The cells were incubated with the PS, and underwent a low-dose PDT to induce apoptosis. After 4 h, the vaccines were generated and the different groups of BALB/c mice were subcutaneously inoculated with 500,000 or 300,000 apoptotic cells. The positive control was subcutaneously vaccinated with 500,000 mitoxantrone (MTX) treated cells. After a week, the mice were challenged with a subcutaneous inoculation of 350,000 viable cells. There was not a statistical significant difference between the treatment groups and the negative control but the vaccines with 500,000 apoptotic cells show some immunogenic effect in tumour growth, comparable to the effect of the MTX vaccines.

ABBREVIATIONS

APC, antigen-presenting cell; ATP, adenosine triphosphate; CRT, calreticulin; DAMP, damage-associated molecular pattern; DC, dendritic cell; DMEM, Dubbelco's modified Eagle's medium; DMSO, dimethyl sulfoxide; DNA, deoxyribonucleic acid; ER, endoplasmic reticulum; F_2BMet, 5,10,15,20-Tetrakis (2,6-fluoro-3-N-methylsulphamoylphenyl) bacteriochlorin; FBS, foetal bovine serum; FWHM, full width at half maximum; HEPES, 4-(2-hydroxyethyl)piperazine-1-ethanesulfonic acid buffer; HMGB1, high mobility group box 1; ICD, immunogenic cell death; LED, light-emitting diode; MHC, major histocompatibility complex; MTX, mitoxantrone; PBS, phosphate-based saline; PenStrep, penicilin-streptomycin; PDT, photodynamic therapy; PI, propidium iodide PS, photosensitizer; ROS, reactive oxygen species; UV, ultraviolet.

INTRODUCTION

Cancer is responsible for one in seven deaths, worldwide, being one of the leading causes of death. In 2012, there were estimated 14.1 million new cases, a number that is expected to keep increasing due to the growth and aging of global population.[1] This pathological process is developed when the normal growth of cells, which is kept under control by inhibitors in the surrounding environment, in the extracellular matrix, and on the surface of neighbouring cells, is disrupted leading to an abnormal growth and spreading.[1,2]

During their evolution to a malign state, tumour cell acquire characteristics that allow tumour growth and metastatic dissemination. They do not need the stimulation of external growth signals, being capable of producing their own; are insensitive to growth suppressors; have pro-survival mechanisms that evade cell death; have limitless replicative potential; can sustain angiogenesis; are able to migrate and invade other tissues. In the last decade, two emerging hallmarks have been added to this list: reprogramming of energy metabolism in order to most effectively support cancer proliferation and evading the immune system.[2]

Photodynamic therapy (PDT) is an established clinical treatment modality for cancer and other non-malignant diseases.[2–5] This technique presents several advantages over the standard anticancer therapies (i.e., surgery, radiotherapy, and chemotherapy) because it is minimally invasive, it has a low mutagenic potential, low systemic toxicity, and it targets specifically the tumour tissue.[2,3,6]

PDT requires only the use of a photosensitizer (PS), light irradiation of a specific wavelength for each PS, and oxygen. These components are harmless individually, but their combination can generate reactive oxygen species (ROS) that are responsible for the destruction of the tumour.[4,5,7–9] The treatment involves the systemic or topical administration of the PS, which accumulates in the tumour tissue that will be irradiated[2,4,10] after an optimized drug-to-light interval. The PS, among other characteristics,[5,7] has to have a high absorption peak between 650 and 850 nm, a range known as the phototherapeutic window (spectral region where the tissues are the most transparent), balancing deeper penetration of tissues (longer wavelengths) with providing enough energy to excite the oxygen to its singlet state (shorter wavelengths). When the PS is irradiated with visible light, the molecule is activated from its ground state to a short-lived single excited state ($^1PS^*$) which can undergo intersystem crossing to form a relatively long-lived excited

triplet state ($^3PS^*$). In type I photochemical processes, the $^3PS^*$ participates in electron or hydrogen-atom transfer reactions with biological substrates to produce radical forms that act as intermediates to generate reactive oxygen species. In type 2 photochemical processes the $^3PS^*$ transfers energy directly to molecular oxygen to form the phototoxic excited-state singlet oxygen ($^1O_2$).[2,6,7,11,12]

The ROS generated by PDT are able to lead to cell death via different pathways, that are not mutually exclusive: autophagy, necrosis, and/or apoptosis.[5,12] Autophagy is a process of degeneration of the macromolecular components of the cytoplasm and organelles, which are surrounded by the autophagosome. Following the merger of the lysosome with autophagosome, its content is degraded.[12] Cell death by autophagy in PDT-treated cells is still controversial, since it plays a role in either inhibiting or stimulating cell death, following the PDT treatment.[2,10,12] Generally, autophagy acts as a pro-survival strategy in cells capable of apoptosis, and promotes cell death in apoptosis-deficient cells.[2] However, it appears that therapy-prompted autophagy in tumour cells has the ability to regulate the release/exposure of multiple danger signals, also called damage-associated molecular patterns (DAMPs; molecules that usually remain inside live cells but are released from or exposed at the surface of dying cells), that are associated to the inflammatory response. The inhibition of this cell death pathway prevents one of these DAMPs: the release of adenosine triphosphate (ATP) by dying cells, showing that autophagy plays an important role in the immune system.[12–14] Necrosis is one of the primary reactions to PDT, observed at cellular level.[15] It consists in a pathological process where the cytosolic contents are spilled to extracellular space due to loss of membrane integrity and complete degradation of the cell.[12,16] This type of cell death takes place above the threshold of resistance of cells treated with non-physiological disturbances, thus it is often observed after PDT with high light and photosensitizer doses.[2,12,16] Typical necrotic changes involve an overload of intracellular Ca^{2+} (from the passive influx caused by damaged membrane, and from the outflow from the endoplasmic reticulum (ER)), activation of many deoxyribonucleic acid (DNA) nucleases, and lysosomal damage, which consequently leads to the total cell lysis.[5,12] The release of the disintegrated organelles results in a strong response from the immune system and the onset of inflammation, and this is why the release of DAMPs was originally connected to this cell death pathway.[12,17] However, the notion that necrosis is immunogenic[16] while apoptotic tumour cells do not show the same effective response in activating the immune system has been invalidated by recent reports.[2,17,18] Apoptosis is the other major cell death caused in response to PDT[5]: a type of programmed cell death responsible for eliminating unwanted cells causing disturbances in their integrity or eliciting inflammatory responses. It is easily recognized by the changes in cellular morphology (shrinkage, blebbing of the membrane, chromatin condensation and DNA fragmentation).[12] Apoptosis is a very complex type of cell death that can occur via different pathways, depending on the cellular organelles involved in the process. The best known mechanisms of apoptosis are the extrinsic (death receptor) and the intrinsic (mitochondrial) pathways.[2,12] The extrinsic pathway operates on the membrane receptors (e.g., tumour necrosis factor receptors) that by binding their respective ligands, induce the activation of caspases. The intrinsic pathway is activated by an increase of ROS, disruption of the ion transport, or the increase of Ca^{2+} in the cytoplasm, leading to the release of pro-apoptotic molecules (e.g., cytochrome c) into the cytoplasm. This release is controlled by proteins of the Bcl-2 family, being favoured when two pro-apoptotic members of the Bcl-2 family, Bax and Bak, are oligomerized and inserted in the mitochondrial membrane. When cytochrome c is in the cytosol it is able to initiate the activation of the cascade of caspases.[2,5,6,12]

However, the efficiency of PDT lies in two other mechanisms, besides the direct cytotoxicity through the types of cell death mentioned above: damage to tumour vasculature that deprives the tumour of oxygen and nutrients, and an acute inflammatory response by recruiting and activating immune cells.[2,4,8,9,11,12,16,19] The standard PDT treatment stimulates inflammation causing a strong immune response that is not only localized at the treatment site, involving both the innate and adaptive immune systems at a systemic level. Innate immunity in response to PDT is characterized by an increased expression of pro-inflammatory cytokines, neutrophil infiltration into the treated tumour site, and activation of the complement cascade.[2,4,10,15,19] This is followed by the activation of the adaptive immune system where PDT enhances the activation and maturation of APCs (dendritic cells (DCs) in particular)[2,4,5,15] that are responsible to phagocytise tumour cells destroyed by PDT, process the tumour-specific peptides, and present them as antigens on their membranes in the context of major histocompatibility complex (MHC) class II molecules. This presentation allows the recognition of the antigens by $CD4^+$ helper T cells that in turn will sensitise $CD8^+$ cytotoxic T cells, as well as the generation of CD4+ and CD8+ memory T cells that will recognize and target tumour-specific antigens leading to immunity.[4,6] It has also been acknowledged the importance of MHC class I molecules, that are found to be downregulated in tumour cells (one of the causes responsible for poor antitumour immunity),[2] for $CD8^+$ cytotoxic T cells to recognize and destroy tumour cells.[2,5]

Furthermore, PDT treatment of tumour cells is able to induce DAMPs that can trigger antigen presenting cells (APCs), which is related to antitumour immunity through the establishment of CD8+ T cell cytotoxic and memory responses, even in the absence of CD4+ T cells.[2,4,5] More attention has been brought to these molecules because of their association with the immunogenicity of dying tumour cells, namely an immunogenic form of apoptosis that presents the same biological hallmarks of "tolerogenic" apoptosis but is able to expose/release DAMPs and elicits an immune response against tumours. This lead to a screening of cytotoxic agents/modalities in cancer treatment that can elicit immunogenic cell death (ICD), in order to develop strategies to reinforcing the therapeutic effect of the treatment.[2,20] The main DAMPs that characterize ICD are the exposure of calreticulin (CRT) on the membrane, the translocation to the membrane's surface or extracellular release of heat shock proteins, release of the high mobility group box 1 (HMGB1) and other end-stage degradation products (e.g., ATP), and secretion of inflammatory cytokines.[2,10,17,21] However, it is accepted that a tumour cell subjected to a cancer treatment undergoes ICD, if there is subsequent CRT exposure, HMGB1 release, and ATP secretion.[10,12,14,18,20]

CRT is a Ca^{2+}-binding protein mainly located in the ER lumen acting in the correct folding of proteins, regulation of Ca^{2+} homeostasis, and signalling. It is also responsible in the assistance of the proper assemble of MHC class I molecules and the load of antigen, along with other functions outside the ER like regulation of nuclear transport and cell proliferation and migration. When CRT is translocated to the membrane and exposed on the surface of tumour cells undergoing ICD, it acts as an "eat-me" signal and simplifies their engulfment by DCs leading to tumour antigen presentation and tumour-specific $CD8^+$ cytotoxic T cell responses.[2,17,20] HMGB1 is an abundant nuclear non-histone chromatin-

binding protein. It affects several nuclear functions such as DNA repair and recombination, stabilization of nucleosomes, and transcription, but HMGB1 also has cytosolic[17] and extracellular[17,20] roles, where it mediates autophagy and acts as a secreted cytokine (not as DAMP), respectively. It is accepted that when a cancer treatment induces ICD, dying tumour cells release HMGB1 causing an intense inflammatory response by stimulating the production of pro-inflammatory cytokines from innate immune cells but the specific role of HMGB1 in ICD is still unclear. Recent studies claim that these multiple behaviours might be influenced by the redox state of HMGB1, which changes its activity between chemoattractant DAMP (fully reduced HMGB1), pro-inflammatory cytokine-inducing DAMP (disulphide bond-possessing HMGB1), and inactivated DAMP (fully oxidized HMGB1; it still maintains chemoattractant properties). However, it is worth of note that HMGB1 reducible states can also interfere with antitumour immunity through its involvement in tumour tissue invasion and metastasis, in decreasing antitumour immunogenicity, and in promoting resistance to chemotherapeutics and irradiation.[2,17,20] The extracellular release of ATP (a nucleotide usually found in the ER) modulates different cellular functions (i.e. survival, death, adhesion, proliferation, differentiation, and mobility) but it is well known as a "find-me" signal that can be secreted through several mechanisms by dying cells which attracts APCs. The presence of extracellular ATP on the cell surface is also responsible for the regulation of DC migration, and activation of antitumour immune responses.[2,17]

To elicit ICD, the combined action of two components is required in order to trigger the intracellular mechanisms: production of ROS and ER stress.[10,17,21] The ER is an eukaryotic organelle responsible for vital sensing, biosynthetic and signalling functions, as well as for the synthesis, folding and post-translational modifications of a large of number of proteins. If the ER homeostasis is disturbed, it causes an imbalance between protein folding load and capacity: this is termed ER stress. The first response is activating a pro-survival pathway that tries to restore the homeostasis but when the ER stress is too severe that pathway turns into one of pro-death.[17]

This combination suggested that PDT treatments had the potential to induce a strong immune response through ICD.[10,17,21] And that was in fact the case, though most research on PDT-induced DAMP exposure used Photofrin as a PS, Garg *et al.*[22] published one of the most important discoveries in the field of ICD.[22,23] They investigated the exposure of DAMPs using PDT with hypericin, a PS which associates with the ER membranes, and the results obtained showed the first type II ICD inducer described in the literature.[22] Treatments that induce primary ER stress are known as type II inducers and show a stronger immune response compared to treatments that induce ER stress as secondary effect through damage to other cellular targets (type I ICD inducers).[10,17] In PDT, the ER stress can be modulated with the use of a PS that localizes preferably in the ER, that when excited causes a massive production of ROS (focused ROS-based ER stress), inducing ICD.[7,17]

One of the most interesting developments that resulted from the continued investigation for improved efficacy and expanded use of PDT is to exploit this immune response in the generation of antitumour vaccines.[3,24,25] Vaccines contain agents incapable of harming the host but able to trigger an immune response by boosting the immune system's natural ability to protect and defend the body against infections or dangers from growth of abnormal cells, as is the case of antitumour vaccines. These are considered to be therapeutic,[3,26,27] if they act as treatment of an existing cancer, like a recent vaccine approved by the FDA to treat metastatic prostate cancer; or are prophylactic,[24] if their aim is to prevent the development of cancer in healthy individuals, such as a vaccine that is against human papilloma virus, and other vaccine against hepatitis B virus. [25,28] Antitumour vaccines have minimal toxicity and offer different strategies that target the immune system,[29] being able to use: DC that are able to express immunostimulatory cytokines in parallel with antigen presentation;[29,30] tumour-associated antigens as therapeutic targets (peptide-based vaccines) inoculated with an appropriate adjuvant;[29,31] or viral/plasmid DNA vectors that deliver antigens or antigen fragments (genetic vaccines);[29] and tumour cells (autologous or allogeneic) that are usually subjected to lethal doses of radiation, or tumour cell lysates, to inoculate the antigens exposed on the surface of the cells for tumour-specific immunization;[26,29,32,33] In this last type of antitumour vaccines it is important to say that most tumour cells are poorly immunogenic, and may not be able to stimulate the immune system as expected.[16]

Nevertheless, PDT is able to increase the immunogenicity of these cells through induction of ICD and the development of PDT-generated vaccines[3,24,26] is a promising strategy to enhance immunostimulation to the level of systemic PDT,[15] and proves to be more advantageous over antitumour vaccines generated through X-ray exposure, ultraviolet (UV) irradiation, hyperthermia, or freeze-thaw lysates, due to the highly amplified immunogenicity triggered by DAMPs.[2,5]

Our work explores the possibility of generating a prophylactic antitumour vaccine using PDT. The PS used was a halogenated bacteriochlorin recently described (5,10,15,20-Tetrakis (2,6-fluoro-3-N-methylsulphamoylphenyl) bacteriochlorin, or F_2BMet)[7–9] named redaporfin (that highly localizes in the ER) to evaluate its immunogenicity. Previous work in our group with redaporfin showed a systemic immune response in the control of metastasis[34] in BALB/c mice. Thus, it was of interest to seek ways of developing strategies that potentiate systemic PDT using redaporfin. To assure a greater coverage of potential antigens the protocols developed during this project are intended to generate whole-cell vaccines with homogeneous populations of cell death (apoptotic or necrotic), and assess which method will be able to better stimulate the immune system of BALB/c mice against a tumour challenge.

EXPERIMENTAL SECTION

Reagents

The growth media for cell culture used were RPMI-1640 media (purchased from Sigma-Aldrich) and Dubbelco's Modified Eagle's Medium (DMEM; purchased from Sigma-Aldrich), for 4T1 cell line and CT26 cell line, respectively. Both media were supplemented with 4-(2-hydroxyethyl)piperazine-1-ethanesulfonic acid buffer (HEPES) 10 mM, and sodium bicarbonate 10mM, purchased from Sigma-Aldrich. Foetal bovine serum (FBS) and penicillin-streptomycin (PenStrep) were purchased from Gibco. Milli-Q water was deionised with a Millipore Milli-Q water purification system.

Potassium phosphate dibasic, potassium chloride, sodium phosphate dibasic, and sodium chloride were purchased from Sigma-Aldrich and used to prepare the phosphate-buffered saline (PBS) solution. PBS Ca/Mg was supplemented with calcium chloride dehydrate and magnesium chloride hexahydrate, also purchased from Sigma-Aldrich.

Trypsin-EDTA solution (10x), Trypan Blue, dimethyl sulfoxide (DMSO), and Propidium Iodide (PI; ≥ 94%) were

purchased from Sigma-Aldrich. Hoechst 33342 stain was purchased from Life Technologies.

Redaporfin (Supplementary Figure 1A) was kindly provided by Luzitin, SA. Mitoxantrone (MTX; Supplementary Figure 1B) was purchased from Sigma-Aldrich.

Equipment

All the procedures dealing with the manipulation of cells, growth media, PBS solutions, and other reagents and materials were performed in a Thermo Scientific MSC-Advantage laminar flow hood.

All weight measurements were made at room temperature on a previously calibrated Kern ALJ 220-5DNM analytical balance.

Culture flasks, cell scrapers, conical centrifuge tubes, micropipettors, and ComfoPette used were purchased from Orange Scientific. Glass Pasteur pipettes, standard tips, and 1.5 mL/2.0 mL tubes were purchased from Frilabo. The material used to deal with cells was previously sterilised in the AJC Uniclave 88 autoclave, before entering the hood environment.

An Olympus CKX41 inverted microscope equipped with an Olympus U-RFLT50 power supply unit was used to observe cell morphology and fluorescent dyes to assess cell viability.

Absorption spectra of redaporfin stock samples were recorded in UV-visible Recording Spectrophotometer (Shimadzu). The samples were measured in quartz cuvettes with an optical path of 1 cm.

The light source used was a light-emitting diode (LED) from Marubeni (model L740-66-60-550), with an output power of 410 μW, emission maximum at 740 nm with FWHM = 25 nm. The fluence of the LED was verified with a Coherent LaserCheck power meter, choosing a wavelength of 749 nm with the filter position on "< 10 μW".

Preparation of redaporfin stock solution

The 1mM stock solution of redaporfin (Supplementary Figure 1A) was prepared by dissolving 1.70 mg of redaporfin in 1.5 mL of DMSO and subjected to 35 kHz in a Bandelin Sonorex TK52 ultrasonic bath for 30 s to avoid the formation of clusters.

The concentration of the stock solution was calculated through its absorption spectra (Supplementary Figure 2) using the Beer-Lambert Law (equation 1):

$$(1) \qquad A = \varepsilon \, l \, c$$

where: A is the absorbance at the peak position, ε (cm^{-1} M^{-1}) is the molar attenuation coefficient, l (cm) is the path length, and c (mol/L or M) is the molar concentration of the Redaporfin sample. The molar absorption coefficient is ε_{749}=1.21x10^5 cm^{-1} M^{-1} and the path length is 1 cm. The molar concentration of the stock is obtained when multiplying the molar concentration of the sample by the dilution factor of the sample from the stock solution in DMSO. A DMSO sample was used as a "blank".

The stock solution was kept refrigerated, at 4ºC, protected from light exposure.

Preparation of MTX stock solution

The 1 mM stock solution of MTX was prepared by dissolving 1.03 mg of MTX in 2 mL of PBS, and stirred. The stock solution was kept refrigerated, at 4ºC.

Cell culture

The cell lines used were 4T1mouse mammary tumour cells and CT26 mouse colon carcinoma cells. 4T1 cells were cultured in RPMI medium supplemented with 10% of FBS and 1% of PenStrep, and CT26 cells were cultured in DMEM medium supplemented with 10% of FBS and 1% of PenStrep. Both growth media were prepared as described in the Supplementary Information. The cells were grown in sterile T75 flasks with filter cap in the Thermo Scientific BB15 incubator, at 37ºC in a humidified environment containing 5% carbon dioxide (CO_2). The cells' growth was maintained for 2 to 3 days; when the cells reached 80% confluence, they were detached with Trypsin.

In vitro PDT of 4T1 cells

The vaccines were generated based on the procedures described by Korbelik *et al.*[3] and Garg *et al.*,[18] with some modifications. Firstly, 1.00x10^6 4T1 cells were seeded in T75 flasks with 10 mL of growth medium, and left to incubate overnight so the cells could adhere to the flask. The following day, the medium was removed and replaced with 15 mL of the solution of redaporfin in growth medium in the required concentration.

The PS was incubated for 18-20 h before it was removed, and the cells were washed twice with 5 mL of PBS to remove the excess of redaporfin that was not internalized by the cells. After washing the cells, 10 mL of growth medium was added to the cells that were then exposed to the LED light for a calculated time interval (Δt) until it achieved the intended light dose, using equation 2. Higher light doses were used to induce necrotic cell death and lower light doses were used to induce apoptotic cell death.[2,34,35]

$$(2) \qquad \underset{\text{dose}}{\text{Light}} \left(\frac{\text{J}}{\text{cm}^2}\right) = \underset{\text{rate}}{\text{Fluence}} \left(\frac{\text{W}}{\text{cm}^2}\right) \times \Delta t \, (\text{s})$$

The cells were left to incubate for 24h, and then were subjected to an additional procedure before generating the whole-cell vaccines (Supplementary Scheme 1A).

Additional procedure

X-ray irradiation. An experiment with 300,000 live cells was conducted to see if the conditions of X-ray irradiation available were viable to increase cell death. The cells were collected with the growth medium and were centrifuged at 3,000 rpm for 8 minutes. Then, the supernatant was removed and the cells were washed in 2 mL of PBS, followed by another centrifugation at 3,000 rpm for 5 minutes. Afterwards, the supernatant was discarded, and the cells were redispersed in 100 μL of PBS and transferred to a 200 μL tube in order to be centrifuged again at 3,000 rpm for 5 minutes. The supernatant was removed leaving the pellet in the tube. The sample was then irradiated by a Philips PW 1830/00 (X-ray generator) with a Mo tube (K_α, λ=0,71073 Å). The generator was operated with the white spectrum of the tube, without filter or monochromator, with a power of 2kW. The tube with the pellet of cells was set in the arrangement displayed in Supplementary Figure 3, while being irradiated with X-rays for 2 h.

UV picosecond irradiation. The cells were scraped off and collected with the growth medium similarly to the protocol for X-ray irradiation. Then the cells were centrifuged and washed with PBS three times, as described in the Supplementary Scheme 1B, to isolate the pellet of treated cells in the tube. The sample was then set in the arrangement displayed in Supplementary Figure 4 while being irradiated by an EKSPLA PL2143A/SH/TH/FH picosecond laser at λ_{em}=266 nm. Cells used for UV control vaccines were administrated redaporfin but were not subjected to PDT. The UV irradiation protocol for these cells suffered some alterations because it involved killing all the cells, needing a higher UV dose: the density of cells irradiated had to be divided in half to be subjected to UV irradiation (Supplementary Scheme 1C). After irradiating, the cells in each tube

were re-dispersed in 100 µL of PBS and the volumes were coupled. Similarly to the test experiment for X-ray irradiation, 300,000 live cells were collected with the growth medium, isolated as described in Supplementary Scheme 1B, irradiated, re-dispersed in RPMI, and left to incubate in a flask to assess cell viability after UV irradiation.

In vitro PDT of CT26 cells

For this protocol, only one type of cell death was induced: apoptosis. Two different cell densities, 1.35×10^6 and 750,000 CT26 cells, were seeded in T75 flasks with 10 mL of growth medium, and left to adhere to the flask by incubating overnight. The next day, the medium was removed and replaced with 15 mL of 5 µM of redaporfin in growth medium.

As described for the *in vitro* PDT of 4T1 cells, the PS was incubated for 18-20 h before it was removed, and the cells were washed twice with 5 mL of PBS Ca/Mg to remove the excess of PS that was not internalized by the cells. After washing the cells, 10 mL of DMEM was added to the cells that were then exposed to 0.35 J/cm^2 of LED irradiation. The time of exposure (Δt) was calculated with equation 2.

The cells incubated for 4 h, then were scraped off the flask and collected with the growth medium to be isolated according to the steps for centrifugation and wash, described in Supplementary Scheme 2B. The pellet of treated cells in the tube was used to generate the vaccines.

Positive control

To compare the immunogenicity of the generated vaccines, we prepared a protocol with a whole-cell vaccine generated with MTX, which is known to induce ICD[17,21].

750,000 CT26 cells, were seeded in T75 flasks with 10 mL of growth medium, and left to incubate overnight. The next day, when the cells adhered to the flask, the growth medium was removed and replaced with 15 mL of a 5 µM solution of MTX in DMEM. The MTX solution was incubated for 24 h.

The cells were then scraped off and collected with the MTX in order to be centrifuged and washed with PBS, four times. This process is represented in detail in Supplementary Scheme 3B. In between centrifugations, it was obtained a blue pellet that contained the cells with internalized MTX (blue). After this process of isolation, the pellet of cells in the tube was used to generate MTX vaccines.

Animals and vaccine protocol

All the *in vivo* studies were performed in BALB/c female mice, in accordance with local ethical guidelines. In each set of experiments, the mice were randomly assigned to four different treatment groups (n=6). Tumour volume was calculated using equation 3.

$$\text{Tumour volume}\,(\text{mm}^3) = \frac{a\,(\text{mm}) \times b^2\,(\text{mm})^2}{2} \quad (3)$$

where: a is the major axis of the tumour, b is the minor axis of the tumour.

The follow-up of the animals for both experiments can be found in the Supplementary Information, starting from the day the vaccine was inoculated (day 0).

4T1. The experiment was performed in 11 to 16-week old mice. In the PDT followed by UV irradiation (Apoptosis/UV or Necrosis/UV) and UV control treatment groups, the animals were vaccinated subcutaneously (using a 21G needle) on the left flank with 3.00×10^6 treated cells re-dispersed in 200 µL of PBS. The negative control group was inoculated subcutaneously on the left flank with 200 µL of PBS. The animals were rested a week and then inoculated subcutaneously (using a 26G needle) on the right flank with a challenge of 350,000 viable 4T1 cells re-dispersed in RPMI without FBS or PenStrep supplements. The animals were sacrificed when the major axis of the tumour reached 1.5 cm, or at 33rd day after vaccination.

CT26. The experiment was performed in 15 to 16-week-old mice. In the PDT treatment groups, PDT_{500} and PDT_{300}, the animals were vaccinated subcutaneously (using a 26G needle) on the left flank with 500,000 and 300,000 treated cells, respectively, re-dispersed in 200 µL of PBS. The MTX treatment group was vaccinated subcutaneously on the left flank with 500,000 treated cells re-dispersed in 200 µL of PBS. The negative control group was inoculated subcutaneously on the left flank with 200 µL of PBS. The animals were rested a week and then inoculated subcutaneously (using a 26G needle) on the right flank with a challenge of 350,000 viable CT26 cells re-dispersed in DMEM without FBS or PenStrep supplements. The animals were sacrificed when the major axis of the tumour reached 1.5 cm, or at 31st day after vaccination.

Statistical analysis

The results for the evaluation of tumour growth are expressed as means ± SEM and statistical difference was analysed with a two-tailed, two-sample Student's t-test with unequal variance, α=0.05.

RESULTS

Modulation of 4T1 cell death with PDT

Several conditions of different PS concentrations and light doses were experimented on 4T1 cells while simulating the *in vitro* PDT protocol described for this cell line.

The type of cell death obtained for all of the different conditions experimented is listed in Supplementary Table 1, ordered from the lowest to highest ROS factor associated (calculated using equation 4).

$$\text{ROS factor} = \text{Light dose}\,(\tfrac{\text{J}}{\text{cm}^2}) \times [\text{Redaporfin}]\,(\mu\text{M}) \quad (4)$$

After assessing which conditions achieved the highest percentage of cell death without losing homogeneity, the experiments with the chosen values for concentration of redaporfin and amount of light dose (see Table 1) were repeated thrice to assure reproducibility. Figure 1 shows the two types of cell death induced, 24 h after PDT.

Table 1. PDT conditions to modulate type of cell death

	[F_2BMet] (µM)	Fluence rate (mW/cm^2)	Light dose (J/cm^2)	Cell death (%)
Apoptosis	1.26	≈ 1.0	0.15	80 – 90
Necrosis	1.26	≈ 2.0	2.00	> 90

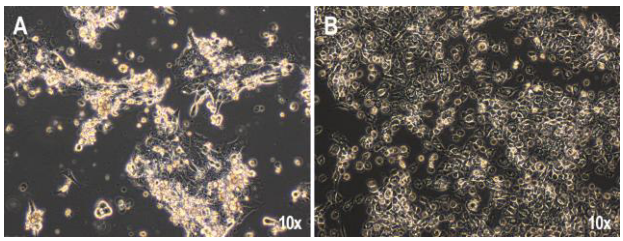

Figure 1.Types of cell death induced by the *in vitro* PDT protocol. (A) Apoptotic cells 24 h after PDT. (B) Necrotic cells 24h after PDT.

Generation of 4T1 whole-cell vaccines

Adapting the method described by Korbelik *et al.*,[3] 24 h following the *in vitro* PDT protocol and before generating the vaccines, the cells were subjected to an additional procedure to increase the percentage of cell death.

The first option experimented was X-ray irradiation. Since the conditions referred in the literature[3] were not available, the procedure was carried out as described in the experimental section. After the X-ray irradiation, the cells were redispersed in RPMI and transferred to a T25 flask to be left to incubate overnight. The next day, when evaluating the flasks it was obvious that there was not a cytotoxic effect, but visibly helped proliferation, as shown in Figure 2. The control group (Figure 2A) underwent the same procedures except the X-ray irradiation, when the cells just remained without growth medium for 2 h (time of the irradiation).

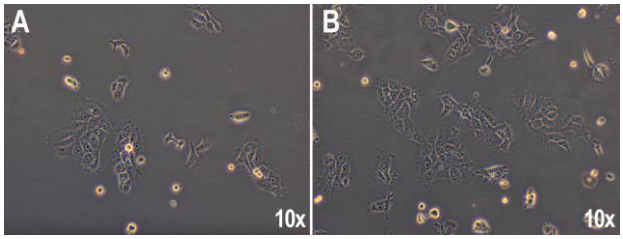

Figure 2. Cell viability 24h after X-ray irradiation. (A) Control group. (B) Cells irradiated for 2h.

The X-ray irradiation was put aside, and replaced with UV irradiation, which is known to induce ICD.[21,24] As described in the experimental section, a test experiment was conducted to assess cell viability after UV picosecond irradiation. The viability of cells which were irradiated for different doses of UV radiation, after 48 h, is shown in Supplementary Figure 5. The effect of UV irradiation is visible in all of the conditions experimented, as high levels of apoptosis. However, there are considerable amounts of viable cells in the lower doses (0.78 and 1.56 J) that decrease when the dose is increased (3.90 J), to a point where no viable cells were found (7.80 and 15.6 J). These values were obtained through equation 5, by varying the time of exposure to UV irradiation.

$$(5) \qquad D_T\,(J) = P\,(W) \times \Delta t\,(s)$$

where: D_T is the total dose of UV radiation that the cells were subjected to, P is the power of the laser (takes into account the energy of one pulse, and that the laser shoots 10 pulses per second), Δt is the amount of time that the cells are irradiated.

After repeating the experiment, simulating the full *in vitro* PDT protocol followed by UV picosecond irradiation (Supplementary Scheme 1A, B), the optimal conditions for the highest amount of cell death were summarized in Table 2. The additional procedure after PDT was able to increase cell death in approximately 10%.

Figure 3 (A, B and C, D) show the viability of 4T1 cells after combining PDT with UV irradiation to generate the vaccines. As mentioned above and seen in Supplementary Figure 5, the type of death induced by UV irradiation is apoptosis. This, however, does not affect to a great extent the homogeneity of the necrotic cell group (see Figure 3) because the PDT protocol had already induced > 90% of cell death (see Table 1).

Table 2. Conditions to generate 4T1 whole-cell vaccines

	PDT			UV	
	[F_2BMet] (μM)	**Fluence rate (mW/cm^2)**	**Light dose (J/cm^2)**	**Total dose (J)**	**Cell death (%)**
Apoptosis / UV	1.26	≈ 1.0	0.15	11.7	90
Necrosis / UV	1.26	≈ 2.0	2.00	11.7	≈ 100
UV control	1.26	0	0	36.0 *	70 – 80

* Sum of the two doses of 18.0 J of irradiation to each half of the 3.00 x 10^6 4T1 cells needed for the vaccine.

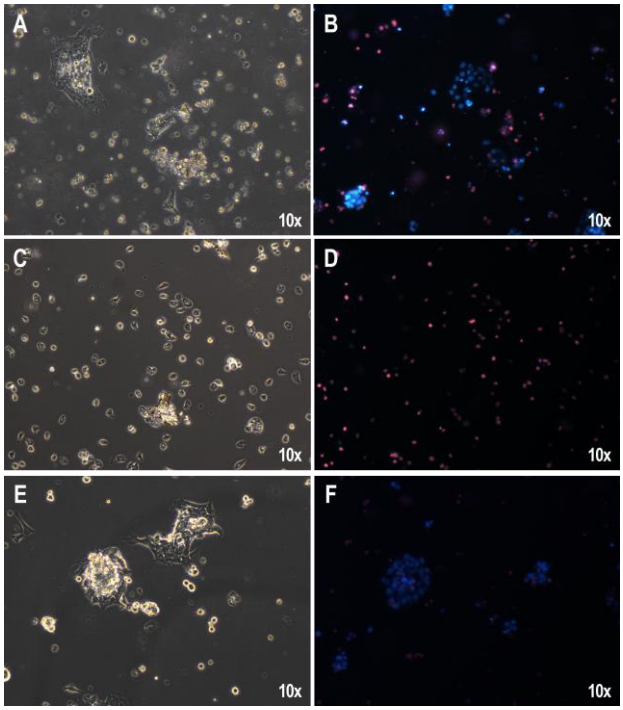

Figure 3. The viability of the different protocols for generating the vaccines. Apoptosis/UV: (A) cells 24h after UV irradiation; (B) stained cells 24h after UV irradiation. Necrosis/UV: (C) cells 24h after UV irradiation; (D) stained cells 24h after UV irradiation. UV control: (E) cells 24h after a total of 36.0 J of UV irradiation; (F) stained cells 24h after a total of 36.0 J of UV irradiation. The fluorescent dyes are Hoechst in blue, and PI in red.

The last type of vaccines generated was the UV control group. These cells were administrated the PS but did not undergo PDT (Supplementary Scheme 1C). After incubating the redaporfin for 18-20 h, the cells were collected and isolated. As all cells were alive, the protocol used for UV irradiation following the PDT was not enough to kill enough cells. So, the UV dose was increased, raising the percentage of cell death as well. The maximum dose experimented was an UV irradiation of 36.0 J (the equivalent to 1 h of irradiation; see Supplementary Figure 6D), achieving a higher rate of cell death. The UV control group obtained the best results in cell death as seen in Figure 3, using the protocol described for UV control in the Experimental section (conditions summarized in Table 2; Supplementary Scheme 1C and Supplementary Figure 6F) for preparing the cells for irradiation, followed by irradiating each half of the total

density of cells for the vaccine with 18.0 J (half the total dose of UV radiation).

In vivo evaluation of the efficacy of PDT-generated 4T1 whole-cell vaccines

To test if our protocol was able to induce immunogenicity and enhance the host antitumour immunity after generating the vaccines as described in the Experimental Section, the animals were inoculated the vaccines (day 0), and after a week they were challenged with 350,000 live cells (day 7). The measurements and statistics of tumour growth for this protocol are displayed in Supplementary Tables 2 – 5. Student's t-test statistical analysis results are summarized in Supplementary Table 6.

After a week of the challenge (day 14), all groups had animals that developed tumours in the challenge site, and the measurement of the tumour sizes revealed that the tumours on the A/UV group were on average smaller than the negative control tumours (see Graphic 1; Supplementary Tables 5 and 2), but N/UV and UV control groups already presented tumours larger than the control ones. On the 21st post-vaccination day, it showed that all the animals in the A/UV, N/UV, and UV control groups showed tumours larger than the control groups indicating that the protocol was not showing the desired effect. This behaviour continued to be visible until the day of the 33rd day endpoint, when the experiment ended and all animals were sacrificed.

Graphic 1. Evaluation of 4T1 tumour growth

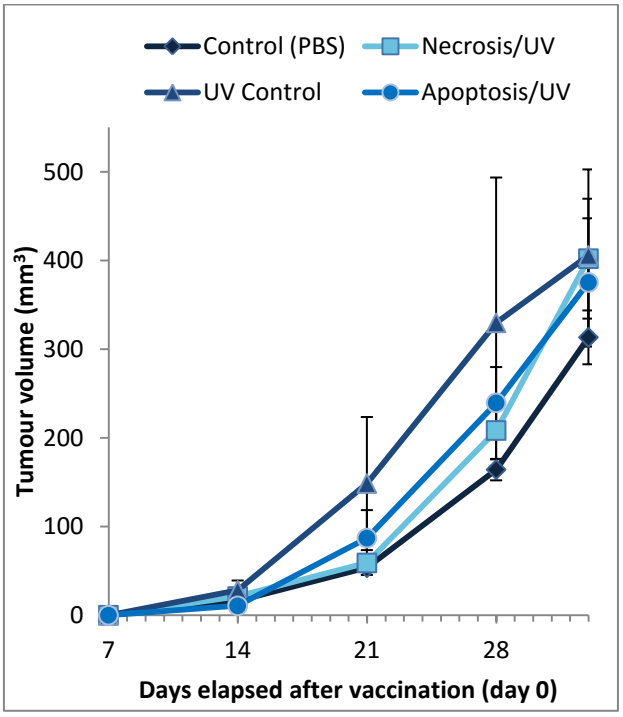

The graphic represents the average tumour growth of the different vaccination groups. The error bars represent the SEM.

The statistical analysis (Supplementary Table 6) showed that despite the difference in averages, there was not a statistical significant difference when compared to the negative control group.

The UV control group always showed the largest tumours in average (Graphic 1) and also the largest SEM (Supplementary Table 3). At the 28th post-vaccination day, four of the mice had already started showing tumour growth on the vaccination site; one of them had developed an intramuscular tumour and reached the endpoint of 1.5 cm on the 27th post-vaccination day. Another one of these mice reached the same endpoint at the 31st post-vaccination day. On the 33rd post-vaccination day, there were four mice, two of them with a tumour growing in the vaccination site.

In the Necrosis/UV group, there were not animals that developed tumours in the left flank (vaccine), and all reached the 33rd day endpoint. In average, the tumours from these animals were always larger than the control tumours but they seemed to grow slower than the other two treatment groups until the 33rd post-inoculation day where it was seen that the tumours were similar in size to the ones from the UV control group.

In the last group of treatment, Apoptosis/UV, the size of the tumours initially appeared to be smaller than the ones in the control group. One week after the challenge (day 14) this was the only group that had two animals which had not developed tumours on the challenge site; however, it already had four mice with tumours on the vaccination site. After 21 days of the vaccination, the average size of the tumours in this group had surpassed the ones in the control and in the Necrosis/UV groups, and all the mice presented tumours on the left flank. One of the mice was sacrificed at the 27th post-vaccination day to avoid unnecessary pain to the animal, since the tumour had invaded the muscle and was affecting its mobility even if the tumour had not reached 1.5cm endpoint. Two other mice were sacrificed 32 days after the vaccine inoculation without reaching any of the endpoints because it was not possible to sacrifice them the next day.

Graphic 2 represents the survival curve of the animals in the different vaccination groups, until the 33rd day endpoint, when all mice were sacrificed and the experiment ended.

Graphic 2. Kaplan-Meier representation of the *in vivo* experiment with 4T1 vaccines

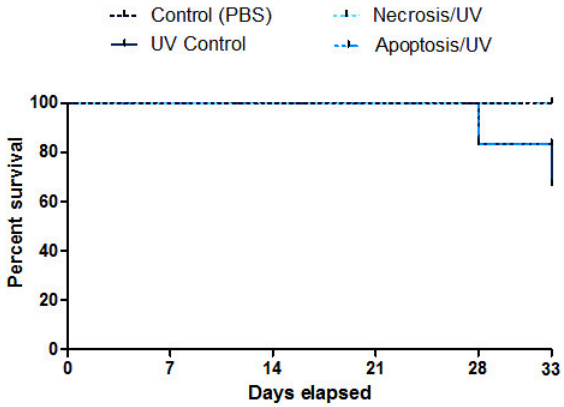

Deaths represented in the different groups were sacrifices of the animals that reached one of the endpoints. At the 33rd day, the experiment ended and all the animals were sacrificed.

Generation of CT26 whole-cell vaccines

For this protocol we decided to study only the effect of apoptotic vaccines because it was the type of cell death that initially showed some difference in tumour growth in the former protocol, and this introduced the possibility of verifying the induction immunogenic apoptosis using PDT. Other change that was introduced was the shortening of post-PDT incubation time to 4 h, since we observed that immunogenicity was lost after 24 h.

We also focused on generating two vaccines with different number of apoptotic cells to see if there was any effect caused by the number of cells used in the vaccine. The *in vitro* PDT conditions for inducing apoptosis in CT26 cells are described in Table 3. The *in vitro* PDT experiments were repeated three times, for both cell densities, and showed that

after 4 h post-PDT it was possible to see 70–80 % of the cells were dead or dying (Figure 4). At this timepoint, the cells were isolated according to the protocol (simplified in Supplementary Scheme 2) to generate the two types of vaccine: PDT_{500}, vaccines with 500,000 cells re-dispersed in 200 µL of PBS; and PDT_{300}, vaccines with 300,000 cells per 200 µL of PBS. Another experiment was conducted to check the viability of these conditions, after 24h (Supplementary Figure 7). This raised the levels of cell death to > 90 %.

The positive control for this experiment was MTX. The cells were incubated 24 h with 5 and 10 µM of MTX dissolved in DMEM to assess cytotoxicity. However, these concentrations resulted in the same 30 to 40 % cell death by apoptosis (Figure 5). Therefore, to generate the vaccines we used a MTX concentration of 5 µM. After the 24h incubation, the cells were isolated according to the protocol (simplified in Supplementary Scheme 3), generating a pellet of CT26 cell with a light blue tint, which showed that the cells had internalized MTX. After the isolation of the pellet with treated cells, the vaccines were generated by re-dispersing 500,000 cells in 200 µL of PBS.

Table 3. Conditions to generate CT26 whole-cell vaccines

	PDT			MTX	
	[F_2BMet] (µM)	Fluence rate (mW/cm^2)	Light dose (J/cm^2)	[MTX] (µM)	Cell death (%)
Apoptosis	4.21	≈ 1.0	0.35		70 – 80
MTX				5	30 – 40

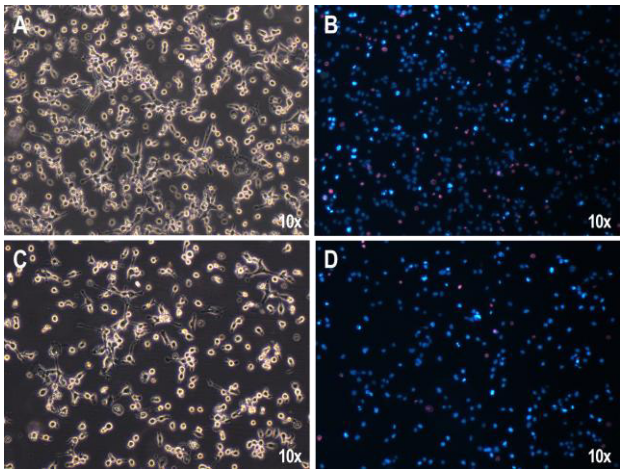

Figure 4. The viability of the different protocols for PDT-generated vaccines. PDT_{500}: (A) cells 4h after PDT protocol; (B) stained cells 4h after PDT protocol. PDT_{300}: (C) cells 4h after PDT protocol; (D) stained cells 4h after PDT protocol.

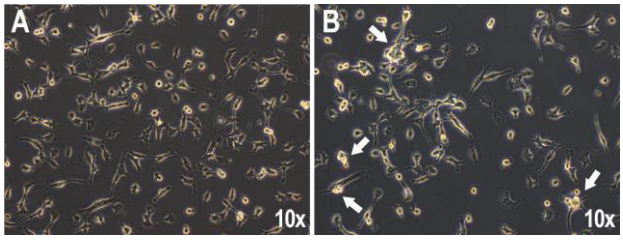

Figure 5. CT26 cells (A) before and (B) 24h after incubation of a 5µM solution of MTX in DMEM. The arrows in (B) indicate the places where the blebbing of the membrane of apoptotic cells is visible.

In vivo evaluation of the efficacy of PDT-generated CT26 whole-cell vaccines

Following the generation of the vaccines, as described in the Experimental Section, the animals from the different groups were inoculated with the vaccines (day 0), and after a week they were challenged with 350,000 live cells (day 7). The evaluation of tumour growth in each group is represented in Graphic 3. The measurements and statistics of tumour growth for this protocol are displayed in Supplementary Tables 7 – 10. Student's t-test statistical analysis results are summarized in Supplementary Table 11.

At the 14th post-vaccination day, all the animals in the control group (n=5) already presented tumour formation, while in the treatment groups only 2 mice had developed tumour from the challenge (Supplementary Tables 7-10). At this point, the tumours from animals in the MTX group were the smallest in average. Overall, the control group was the one with the largest tumours, and 4 out of 5 animals were sacrificed before reaching the end of the experiment (shown in the survival curves represented in Graphic 4), at the 31st post-vaccination day.

Graphic 3. Evaluation of CT26 tumour growth

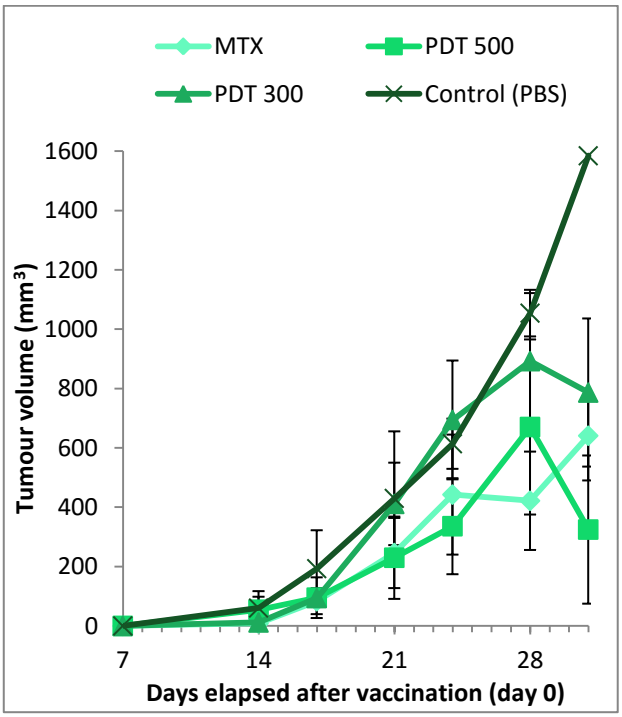

The graphic represents the average tumour growth of the different vaccination groups. The error bars represent the SEM.

The statistical analysis (Supplementary Table 11) showed that there was not a statistical significant difference when the treatments were compared to the negative control group, except for MTX on day 28. This was a single event that was not observed before or after this timepoint.

The group inoculated with the MTX vaccines, was the only group that did not develop a secondary tumour from the vaccination protocol. The tumour growth was always inferior to the control group but it only shows to have statistical significant difference ($p < 0.05$) on the 28th post-vaccination day. On this day, Graphic 3 shows a decrease in the average of tumour growth due to the sacrifice of two of the mice that had reached the 1.5 cm endpoint on day 24. At the end of the experiment 2 out of the 4 mice in this group also reached the 1.5 cm endpoint.

The average tumour growth in PDT_{500} group was very similar to the MTX group, until the 24th post-vaccination day

(Graphic 3) when one mouse from the PDT_{500} group had already been sacrificed (day 21) and two mice from the MTX group reached the 1.5 cm endpoint. The decrease seen after the 28th post-vaccination day in the average of tumour growth of the PDT_{500} group is a result of the sacrifice of two animals that reached the 1.5 cm endpoint on day 28. In this group (n=6), 5 animals developed a secondary tumour in the vaccination site (4 from day 14, and the other from day 21); the mouse which did not develop a tumour from the vaccine was present in the group that reached the end of the experiment (n=3), and was a singularity that did not develop a tumour from the challenge with live CT26 cells (acted as "vaccinated").

The last group of treatment was PDT_{300}. One mouse from this group is not accounted in the statistical analysis, because it developed an intramuscular tumour from the vaccination that reached the 1.5 cm endpoint before the challenge tumour. This made the follow-up of tumour growth unviable to the analysis, and reducing the number of animals in this group (n=5). The growth of the tumour was in average slightly lower to the control group except for the timepoint on day 24, when 2 mice reached the 1.5 cm endpoint and were sacrificed. Tumours caused by the vaccine appeared in 3 out of the 5 animals, on the 14th post-vaccination day. As seen in the other treatment groups, the decrease in tumour growth observed after the 28th post-vaccination day is due to the sacrifice of one mouse that reached the 1.5 cm endpoint. Only 2 out of the 5 animals reached the 31st day endpoint.

Graphic 4. Kaplan-Meier representation of the *in vivo* experiment with CT26 vaccines

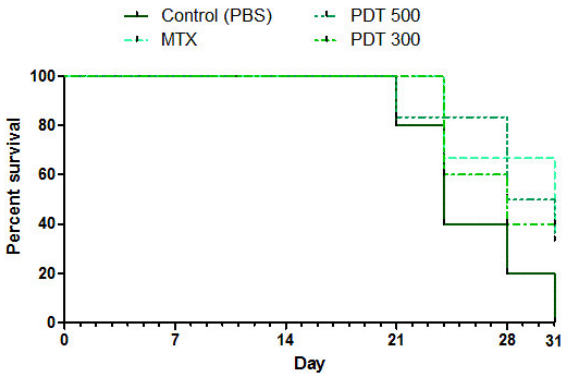

Deaths represented in the different groups were sacrifices of the animals that reached one of the endpoints. At the 31st day, the experiment ended and all the animals were sacrificed.

DISCUSSION

The targeted action of PDT is one of its advantages but it also brings disadvantages when dealing with metastatic lesions.[5] This requires the development of treatments that are able to progress from local to systemic treatments.

PDT is able to produce changes in tumour cells that lead to an increased exposure of surface antigens which are able to stimulate the host immune system[2,4,5] Our group has reported results consistent with this fact using redaporfin, where mice cured with the optimized vascular-PDT protocol were re-challenged 3 months later with CT26 cell in the opposite thigh to the PDT treatment. 67% of the cured mice rejected the re-challenge and remained tumour-free for at least 70 days.[34] Moreover, in the same study Rocha *et al.*[34] disclosed that the PDT protocol also plays an important role in the stimulation of the adaptive immune system.

One of the tasks of this project was to compare the efficiency of apoptosis vs. necrosis in inducing ICD. The first protocol used mice mammary tumour 4T1 cell line which is a highly malignant and very poorly immunogenic.[36] Our group had not yet conducted experiments with this cell line, so we performed experiments with several conditions varying light doses, and PS concentrations in order to modulate the type of cell death. To each combination of redaporfin concentration and light dose we associated a ROS factor, in order to help defining an outcome associated to a dose of PDT. After ordering from the lowest to highest ROS factor (Supplementary Table 1), it was easy to see the "safe" threshold of the combinations that could be used to obtain necrosis (ROS factor ≥ 1.2645) or apoptosis (ROS factor ≤ 0.1897), homogeneously. Using the same concentration of redaporfin (1.26 μM), to induce necrosis it was needed a light dose of 2 J/cm^2 while to induce apoptosis it was used 0.15 J/cm^2. This is concordant to what expected from the literature[2,12,34,35] where necrosis is achieved using higher light doses, and apoptosis is achieved with lower light doses.

Since our purpose was to generate whole-cell vaccines, one of our concerns was having an additional procedure after PDT that excluded the risk of tumour formation because of the vaccine. Korbelik *et al.*[3] used lethal X-ray doses to destroy all viable cells; however, we had not access to the same conditions of X-ray irradiation described in the paper, and had to adapt to the conditions available with an X-ray generator used for crystallography. The conditions used proved to be insufficient in destroying cancer cells, and even seemed to promote cell proliferation. This result might be explained by the observation that mammalian cells have the ability to spontaneously recover from sublethal X-ray damage.[37] Replacing the X-ray irradiation with UV picosecond irradiation, given that UVC radiation (100-290 nm) is identified as an ICD inducer[21,24], we used a picosecond laser emitting in this range (266 nm). With this method we were able to induce apoptosis, which is the expected cell death pathway for UVC irradiation,[21] and increase the cytotoxicity following PDT treatment.

Tumour response to the PDT-generated vaccine was not favourable; the tumour volume in animals inoculated with treated 4T1 cells (PDT/UV and UV control) were in average larger than the ones in the negative control, even if there was not a statistical significant difference. We propose that the loss of immunogenicity of this protocol is due to the 24 h post-PDT incubation previous to generation of the vaccine. The immunogenic signals delivery pattern can be divided in three phases: the decision phase, when CRT is translocated to the membrane within few hours; the processing phase, when HMGB1 is released within 18 h after ICD induction, as well as the release of ATP; and the effector phase, when DCs elicit T cell responses.[2] So, during the post-PDT incubation of 24 h, the immunogenic signals expected to be produced on 4T1 cells by PDT (i.e., presence of DAMPs) may have already been released into the growth medium or destroyed with the cell contents, being discarded later when isolating the cells to generate the vaccines. Furthermore, the additional procedure was unable to eliminate the risk of tumour formation due to the vaccine, in the Apoptosis/UV and UV control groups. The vaccine did not cause tumour development in the Necrosis/UV group but, taking into account the lack of immunogenicity of the vaccines, we suggest that this is a result of the protocol for Necrosis/UV originating near 100% cell death, unlike the former treatment groups.

The analysis from the results obtained, lead to some changes in the protocol. The 4T1 cell line was changed to the mice colon carcinoma CT26 line, which is poorly to moderately immunogenic[34] but less aggressive than the mammary tumour line. The *in vitro* PDT procedure for this cell line was relatively stronger (incubation with 4.21 μM of redaporfin,

and irradiation of 0.35 J/cm^2) supporting the fact that this cell line is more resistant to *in vitro* PDT.[7] Another important alteration to the protocol was the reduction of incubation time after PDT, from 24 h to 4 h. This had the purpose of taking advantage of the spatiotemporal sequence in ICD[2] following PDT, and have already some cytotoxicity to decrease the chance of developing a tumour due to the vaccine.

For this optimized protocol we focused in only inducing apoptosis to generate the vaccines, which was the type of cell death that showed some effect in the beginning of the *in vivo* evaluation of 4T1 whole-cell vaccines, and is the type of treatment-induced cell death known to be associated with ICD.[2,18] This protocol intended to evaluate the efficiency of two different cell densities, 500,000 and 300,000 CT26 treated cells per vaccine, intending to solve the problem of secondary tumour generated by the vaccines. Animals from both groups were still able to develop a tumour in the left flank. Even so, there seems to be a difference between the PDT_{500} group, where besides the single mouse that acted as "vaccinated", all the other animals developed secondary tumour from the vaccine; and the PDT_{300} group where 2 out 5 were did not have tumours caused by vaccination. This indicates that the number of cells in the vaccine is one of the factors to take into account for further optimization: inoculation of smaller number of cells (decrease the chances of generating tumours) more times (increase the vaccine efficiency with a cumulative effect).

The positive control used for comparison was MTX, also known to be immunogenic.[21] We tried to induce the same level of cell death obtained with *in vitro* PDT protocol for CT26 by incubating the cells with 5 μM of MTX for 24 h. However, this was not enough to induce more than 30–40% of CT26 dead/dying cells by apoptosis, which concerned us in term of generating secondary tumours from the vaccine. But after following the *in vivo* experiment, this proved to be the only vaccination group where none of the animals had tumours on the vaccination site. Taking into account that the number of viable cells in these vaccines was clearly superior to the other vaccination groups, this either shows some immunogenic effect in the vaccination site, or it simply means that after 24 h the cells were still dying.

The *in vivo* evaluation of tumour growth in response to the PDT-generated vaccine, while it did not have statistical difference, showed an improvement from the previous protocol with 4T1 cells. Animals that were inoculated with treated CT26 cells (PDT and MTX) were in average smaller than the ones in the negative control. In the PDT_{300} group, the curve of tumour growth did not show much difference when compared with the control group. So even if the smaller number of cells in the vaccines has an effect in the development of secondary tumours in the left flank, the decrease in number of cells also decreased the effect shown by the curve of tumour growth in the PDT_{500} group. PDT_{500} vaccines produced similar results to the MTX vaccines, in the progression of average tumour growth. The results from these vaccination groups seem to be comparable to the work of Korbelik and Sun,[26] though with therapeutic vaccines instead of prophylactic, they were able to generate vaccines that produced differences up to 400 mm^3 between PDT-generated vaccines and untreated controls, in the span of 13 days after treating the tumour. In our protocol, differences of 300 to 400 mm^3 between the PDT_{500} and the control groups can also be seen in the 3rd week after the tumour challenge, proposing that there has some immunogenic effect. The MTX group was the only one to show statistical significant difference to the control group ($p < 0.05$) on day 28. However, this result is not totally accurate because the control group only had a $n = 2$, and this difference was not seen before or after this single event. This behaviour after MTX vaccination is different from what is shown in the study published by Garg *et al.*[18] where ≈ 75% of the mice vaccinated with MTX-treated CT26 cells were able to remain tumour-free during the duration of the experiment (20 – 30 days). This is possibly related to the differences in the protocols to generate the vaccines.

CONCLUSION

In the protocol for PDT-generated 4T1 whole-cell vaccines, the immunogenicity is lost after 24h. Instead of demonstrating a slower tumour growth, the average of tumour volumes of animals from the treatment groups was superior to the ones from the control group. Understanding this loss of immunogenicity allowed us to adjust the protocol by reducing the post-PDT incubation time.

With the protocol for PDT-generated CT26 whole-cell vaccines, the results from the treatment groups showed improvement when compared to the control groups: the average of tumour volumes from treatment groups was lower, indicating the presence of immunogenicity, but not enough to have significant statistical difference. Even if the change to a slightly more immunogenic cell line may have influence in this result, we believe that the decrease of incubation time after *in vitro* PDT held a more important role. By reducing the incubation of 24h to 4h, we were able to vaccinate dead/dying cells in the process of releasing/exposing DAMPs (that was finished *in vivo* after inoculating the vaccine), instead of vaccinating dead cells that had already finished this process *in vitro* and lost the ability to stimulate the mice immune system after inoculation.

This study initiated the optimization of a protocol to generate whole-cell antitumour vaccines using PDT with redaporfin. Although we did not reach an optimal protocol, it has the opportunity to be exploited more thoroughly, and to analyse the possible alterations in type of cell line used, number of cells vaccinated, or post-PDT incubation times, that can still be optimized and combined with other strategies to potentiate systemic PDT.

AUTHOR INFORMATION

Corresponding Author

* Ana I. G. Mata
ana.ig.mata@gmail.com
Department of Chemistry at University of Coimbra
Largo Paço do Conde
3004-531 Coimbra, Portugal

ACKNOWLEDGMENT

It is acknowledged financial support from the Department of Chemistry at University of Coimbra, financially supported by the Fundação para a Ciência e Tecnologia (FCT) with project PEst-OE/QUI/UI0313/2014 and also supported with project PTDC/QUI-QUI/120182/2010. It is also acknowledged all the support from the Structure, Energy and Reactivity group at University of Coimbra, especially Lígia C. Gomes-da-Silva, and Professor Luis G. Arnaut. Additional gratitude is extended to: Luzitin, SA for the gift of redaporfin; Professor José A. Paixão for providing his expert assistance with the X-ray generator; Fábio A. Schaberle for supplying his expert assistance with the picosecond laser; and Hélder T. Soares and Ana Catarina Lobo for the support and assistance with the experiments *in vivo*.

REFERENCES

(1) American Cancer Society. *Global Cancer Facts & Figures*; 3rd ed.; Atlanta: American Cancer Society, 2015.

(2) Panzarini, E.; Inguscio, V.; Dini, L. Immunogenic Cell Death: Can It Be Exploited in PhotoDynamic Therapy for Cancer? *Biomed Res. Int.* **2013**, *2013*.

(3) Korbelik, M.; Stott, B.; Sun, J. Photodynamic Therapy-Generated Vaccines: Relevance of Tumour Cell Death Expression. *Br. J. Cancer* **2007**, *97*, 1381–1387.

(4) Gollnick, S. O.; Brackett, C. M. Enhancement of Anti-Tumor Immunity by Photodynamic Therapy. *Immunol. Res.* **2010**, *46*, 216–226.

(5) Agostinis, P.; Berg, K.; Cengel, K. A.; Foster, T. H.; Girotti, A. W.; Gollnick, S. O.; Hahn, S. M.; Hamblin, M. R.; Juzeniene, A. Photodynamic Therapy of Cancer: An Update. *CA Cancer J Clin* **2011**, *61*, 250–281.

(6) Dougherty, T. J.; Gomer, C. J.; Henderson, B. W.; Jori, G.; Kessel, D.; Korbelik, M.; Moan, J.; Peng, Q. Photodynamic Therapy. *J. Natl. Cancer Inst.* **1998**, *90*, 889–905.

(7) Arnaut, L. G.; Pereira, M. M.; Dąbrowski, J. M.; Silva, E. F. F.; Schaberle, F. A.; Abreu, A. R.; Rocha, L. B.; Barsan, M. M.; Urbańska, K.; Stochel, G.; et al. Photodynamic Therapy Efficacy Enhanced by Dynamics: The Role of Charge Transfer and Photostability in the Selection of Photosensitizers. *Chemistry (Easton).* **2014**, *20*, 1–13.

(8) Krzykawska-Serda, M.; Dąbrowski, J. M.; Arnaut, L. G.; Szczygieł, M.; Urbańska, K.; Stochel, G.; Elas, M. The Role of Strong Hypoxia in Tumors after Treatment in the Outcome of Bacteriochlorin- Based Photodynamic Therapy. *Free Radic. Biol. Med.* **2014**, *73*, 239–251.

(9) Saavedra, R.; Rocha, L. B.; Dabrowski, J. M.; Arnaut, L. G. Modulation of Biodistribution, Pharmacokinetics, and Photosensitivity with the Delivery Vehicle of a Bacteriochlorin Photosensitizer for Photodynamic Therapy. *ChemMedChem* **2014**, *9*, 390–398.

(10) Brodin, N. P.; Guha, C.; Tome, W. A. Photodynamic Therapy and Its Role in Combined Modality Anticancer Treatment. *Technol. Cancer Res. Treat.* **2015**, *14*, 355–368.

(11) Triesscheijn, M.; Baas, P.; Schellens, J. H. M.; Stewart, F. A. Photodynamic Therapy in Oncology. *Oncologist* **2006**, *11*, 1034–1044.

(12) Dąbrowski, J. M.; Arnaut, L. G. Photodynamic Therapy (PDT) of Cancer: From Local to Systemic Treatment. *Photochem. Photobiol. Sci.* **2015**.

(13) Garg, A. D.; Maes, H.; Romano, E.; Agostinis, P. Autophagy, a Major Adaptation Pathway Shaping Cancer Cell Death and Anticancer Immunity Responses Following Photodynamic Therapy. *Photochem. Photobiol. Sci.* **2015**, *14*, 1410–1424.

(14) Kroemer, G.; Galluzzi, L.; Kepp, O.; Zitvogel, L. Immunogenic Cell Death in Cancer Therapy. *Annu. Rev. Immunol.* **2013**, *31*, 51–72.

(15) Mroz, P.; Hashmi, J. T.; Huang, Y.-Y.; Lange, N.; Hamblin, M. R. Stimulation of Anti-Tumor Immunity by Photodynamic Therapy. *Expert Rev Clin Immunol* **2011**, *7*, 75–91.

(16) Castano, A. P.; Mroz, P.; Hamblin, M. R. Photodynamic Therapy and Anti-Tumour Immunity. *Nat. Rev. Cancer* **2006**, *6*, 535–545.

(17) Krysko, D. V; Garg, A. D.; Kaczmarek, A.; Krysko, O.; Agostinis, P.; Vandenabeele, P. Immunogenic Cell Death and DAMPs in Cancer Therapy. *Nat. Rev. Cancer* **2012**, *12*, 860–875.

(18) Garg, A. D.; Krysko, D. V; Verfaillie, T.; Kaczmarek, A.; Ferreira, G. B.; Marysael, T.; Rubio, N.; Firczuk, M.; Mathieu, C.; Roebroek, A. J. M.; et al. A Novel Pathway Combining Calreticulin Exposure and ATP Secretion in Immunogenic Cancer Cell Death. *EMBO J.* **2012**, *31*, 1062–1079.

(19) Castano, A. P.; Mroz, P.; Wu, M. X.; Hamblin, M. R. Photodynamic Therapy plus Low-Dose Cyclophosphamide Generates Antitumor Immunity in a Mouse Model. *Proc. Natl. Acad. Sci. U. S. A.* **2008**, *105*, 5495–5500.

(20) Krysko, O.; Løve Aaes, T.; Bachert, C.; Vandenabeele, P.; Krysko, D. V. Many Faces of DAMPs in Cancer Therapy. *Cell Death Dis.* **2013**, *4*, e631.

(21) Vliet, A. R. Van; Martin, S.; Garg, A. D.; Agostinis, P. The PERKs of Damage-Associated Molecular Patterns Mediating Cancer Immunogenicity: From Sensor to the Plasma Membrane and beyond. *Semin. Cancer Biol.* **2015**, 1–12.

(22) Garg, A. D.; Krysko, D. V.; Vandenabeele, P.; Agostinis, P. Hypericin-Based Photodynamic Therapy Induces Surface Exposure of Damage-Associated Molecular Patterns like HSP70 and Calreticulin. *Cancer Immunol. Immunother.* **2012**, *61*, 215–221.

(23) Adkins, I.; Fucikova, J.; Garg, A. D.; Agostinis, P.; Špíšek, R. Physical Modalities Inducing Immunogenic Tumor Cell Death for Cancer Immunotherapy. *Oncoimmunology* **2015**, *3*, e968434.

(24) Gollnick, S. O.; Vaughan, L.; Henderson, B. W. Generation of Effective Antitumor Vaccines Using Photodynamic Therapy. *Cancer Res.* **2002**, *62*, 1604–1608.

(25) Korbelik, M. Cancer Vaccines Generated by Photodynamic Therapy. *Photochem. Photobiol. Sci.* **2011**, 664.

(26) Korbelik, M.; Sun, J. Photodynamic Therapy-Generated Vaccine for Cancer Therapy. *Cancer Immunol. Immunother.* **2006**, *55*, 900–909.

(27) Korbelik, M.; Merchant, S. Photodynamic Therapy – Generated Cancer Vaccine Elicits Acute Phase and Hormonal Response in Treated Mice. *Cancer Immunol. Immunother.* **2012**.

(28) Frazer, I. H.; Lowy, D. R.; Schiller, J. T. Prevention of Cancer through Immunization: Prospects and Challenges for the 21st Century. *Eur. J. Immunol.* **2007**, *37*, 148–155.

(29) Guo, C.; Manjili, M. H.; Subjeck, J. R.; Sarkar, D.; Fisher, P. B.; Wang, X. Y. Therapeutic Cancer Vaccines. Past, Present, and Future. *Adv. Cancer Res.* **2013**, *119*, 421–475.

(30) Van Brussel, I.; Berneman, Z. N.; Cools, N. Optimizing Dendritic Cell-Based Immunotherapy: Tackling the Complexity of Different Arms of the Immune System. *Mediators Inflamm.* **2012**, *2012*.

(31) Kadowaki, N.; Kitawaki, T. Recent Advance in Antigen-Specific Immunotherapy for Acute Myeloid Leukemia. *Clin. Dev. Immunol.* **2011**, *2011*.

(32) Sinkovics, J. G.; Horvath, J. C. Vaccination against Human Cancers (review). *Int. J. Oncol.* **2000**, *16*, 81–177.

(33) Korbelik, M. Cancer Vaccines Generated by Photodynamic Therapy. *Photochem. Photobiol. Sci.* **2011**, *10*, 664–669.

(34) Rocha, L. B.; Gomes-da-silva, L. C.; Dąbrowski, J. M.; Arnaut, L. G. Elimination of Primary Tumours and Control of Metastasis with Rationally Designed Bacteriochlorin Photodynamic Therapy Regimens. *Eur. J. Cancer* **2015**.

(35) Sur, B. W.; Nguyen, P.; Sun, C. H.; Tromberg, B. J.; Nelson, E. L. Immunophototherapy Using PDT Combined with Rapid Intratumoral Dendritic Cell Injection. *Photochmistry Photobiol.* **2008**, *84*, 1257–1264.

(36) Chen, L.; Huang, T.; Meseck, M.; Mandeli, J.; Fallon, J.; Woo, S. L. C. Rejection of Metastatic 4T1 Breast Cancer by Attenuation of Treg Cells in Combination with Immune Stimulation. *Mol. Ther. J. Am. Soc. Gene Ther.* **2007**, *15*, 2194–2202.

(37) Mauro, F.; Elkind, M. M. Comparison of Repair of Sublethal Damage in Cultured Chinese Hamster Cells Exposed to Sulfur Mustard and X-Rays. *Cancer Res.* **1968**, *28*, 1156–1161.

SUPPLEMENTARY INFORMATION

Preparation of the reagents

RPMI growth medium

The RPMI growth medium is the recommended growth medium for the 4T1 cell line. It was prepared by dissolving 10.4 g of RPMI-1640, 2.4 g of HEPES, and 2.0 g of sodium bicarbonate in 890 mL of milli-Q water supplemented with 100 mL of previously inactivated FBS (10%) and 10 mL of PenStrep (1%), per litre. The mixture was stirred until a homogeneous solution was obtained. Solution was filtered, inside the laminar hood, through a nitrocellulose filter (GVS Life Science) with a porosity of 0.2 μm. RPMI was kept refrigerated, at 4ºC.

DMEM growth medium

The DMEM growth medium is the recommended growth medium for the CT26 cell line. It was prepared by dissolving 13.4 g of DMEM, 5.96 g of HEPES, and 3.7 g of sodium bicarbonate in 890 mL of milli-Q water supplemented with 100 mL of previously inactivated FBS (10%) and 10 mL of PenStrep (1%), per litre. The mixture was stirred until a homogeneous solution was obtained. Solution was filtered, inside the laminar hood, through a nitrocellulose filter (GVS Life Science) with a porosity of 0.2 μm. DMEM was kept refrigerated, at 4ºC.

PBS

A stock of PBS (10x) was prepared by dissolving 1.0 g of potassium phosphate dibasic, 1.0 g of potassium chloride, 5.75 g of sodium phosphate dibasic, and 40.0 g of sodium chloride in 500 mL of milli-Q. PBS (10x) was stored at room temperature.

The PBS solution was prepared from the dilution of PBS (10x) in milli-Q water. PBS was filtered, inside the laminar hood, through a nitrocellulose filter (GVS Life Science) with a porosity of 0.2 μm. PBS was kept refrigerated, at 4ºC.

To prepare PBS Ca/Mg (used to wash CT26 cell between passages), the PBS solution was supplemented with 0.133 g of calcium chloride dehydrate and 0.1 g of magnesium chloride hexahydrate, before filtering the solution. PBS Ca/Mg was kept refrigerated, at 4ºC.

Trypsin solution

Trypsin solution (1x) was used to detach cells for passaging. It was prepared by diluting the Trypsin-EDTA solution 10x (obtained from Sigma-Aldrich) in PBS. Trypsin was kept refrigerated, at 4ºC.

FBS inactivation

Thaw the FBS solution at room temperature, and complete the process in a water bath at 37ºC for 10 minutes. Afterwards, inactivate the serum at 56ºC for 30 minutes, taking into account that all the serum has to be at 56ºC and that it needs to be stirred 4x times during the inactivation. Then, in a sterile environment, the inactivated FBS is divided and transferred in smaller volumes into several conical tubes which would be stored at -20ºC.

Trypan Blue dye

Trypan Blue dye solution was used to determine cell density by discriminating viable cells (white round appearance) from dead cells (dyed blue), since the dye presents a strong blue colour that only colours cells with damaged membrane. The dye solution was prepared by dissolving 40 mg of Trypan Blue purchased from Sigma-Aldrich in 10 mL of PBS solution, and then filtering the solution in a sterile environment. Trypan Blue was stored at room temperature.

Figures and Schemes

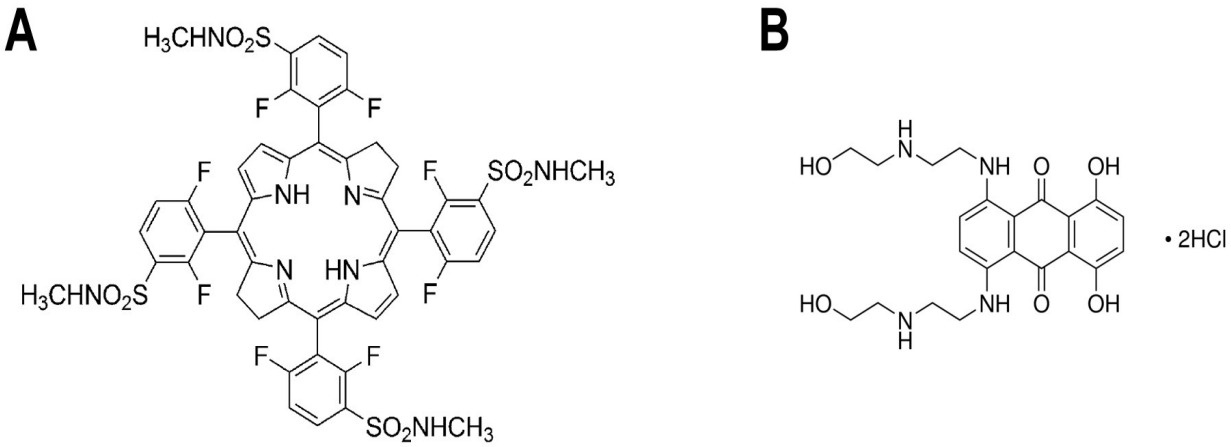

Figure 1. Molecular structure of: (A) the photosensitizer redaporfin (adapted from Krzykawska *et al.*), and (B) MTX (adapted from the Sigma-Aldrich website, http://www.sigmaaldrich.com/catalog/product/sigma/m6545?lang=pt&region=PT; last visited at 13h30, on the 25th of August, 2015).

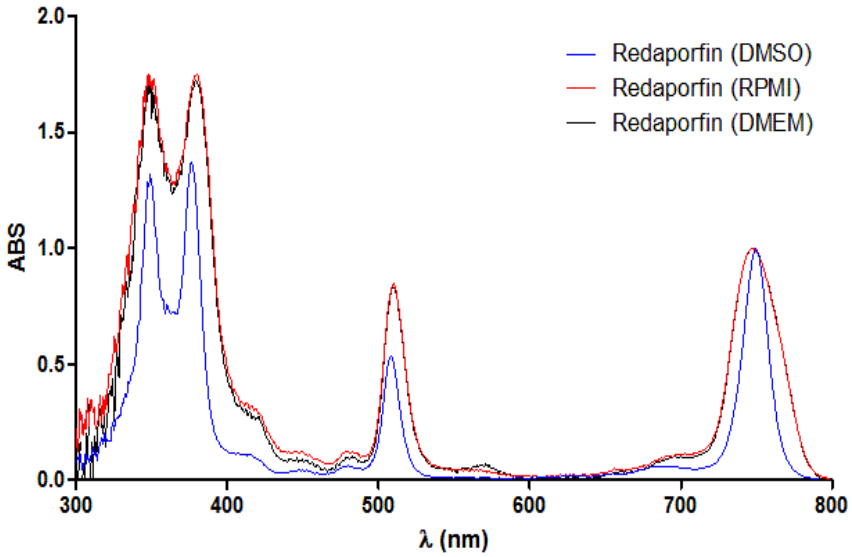

Figure 2. Normalized absorption spectra of redaporfin in the different solvents used during the project.

Scheme 1. Schematic representation of the steps used to generate the 4T1 whole-cell vaccines

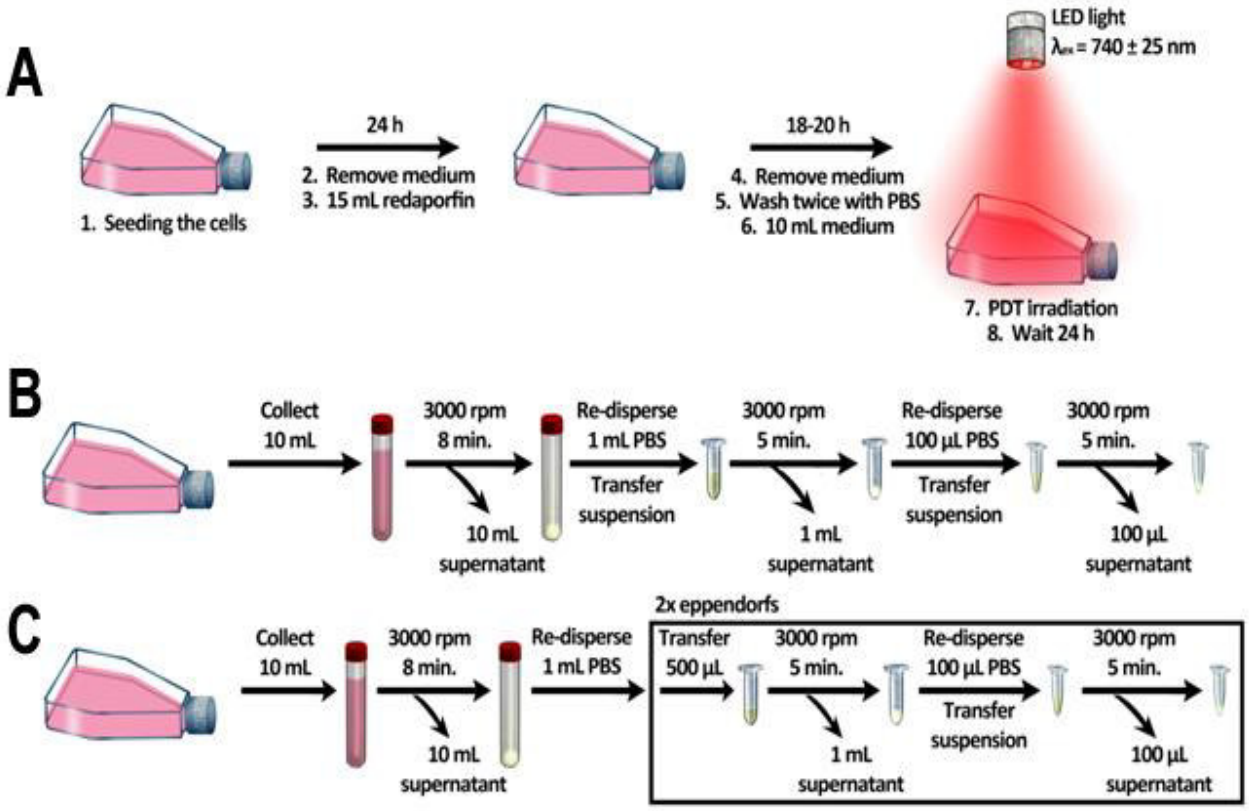

(A) *In vitro* PDT protocol. (B) Protocol to isolate apoptotic/necrotic cells after PDT, for the UV irradiation. (C) Protocol to isolate cells that followed the steps 1-6 from Scheme 1A, for the UV irradiation – UV control group.

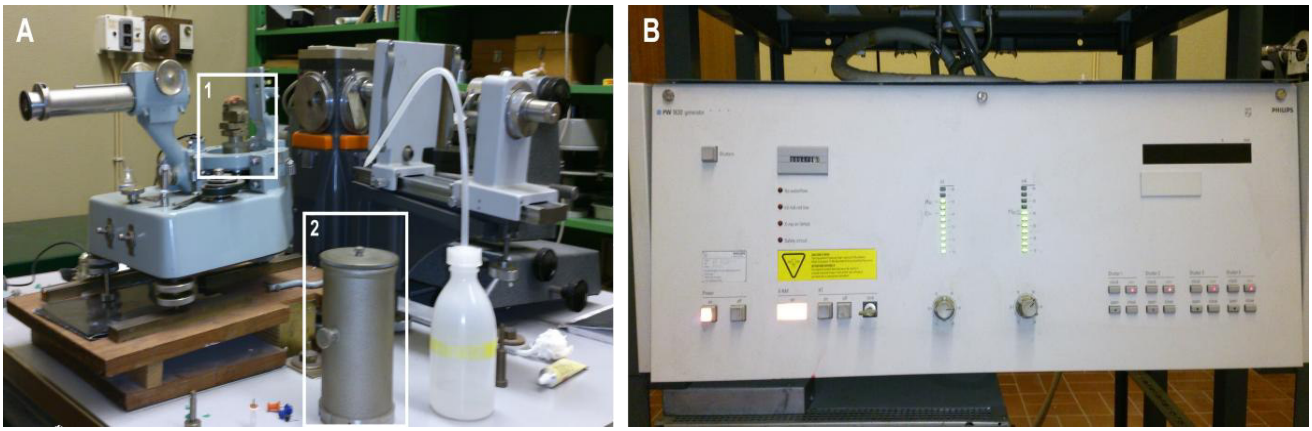

Figure 3. (A) Structure improvised to irradiate the cells using the X-ray generator. The tube containing the pellet of 4T1 cells was glued to the head of a tack, which in turn was attached to a piece of plasticine (placed as seen in A.1) to ensure that the cells had enough height to be in the path of the X-ray irradiation, and then covered with piece A.2. (B) The X-ray generator working at the conditions used for the irradiation.

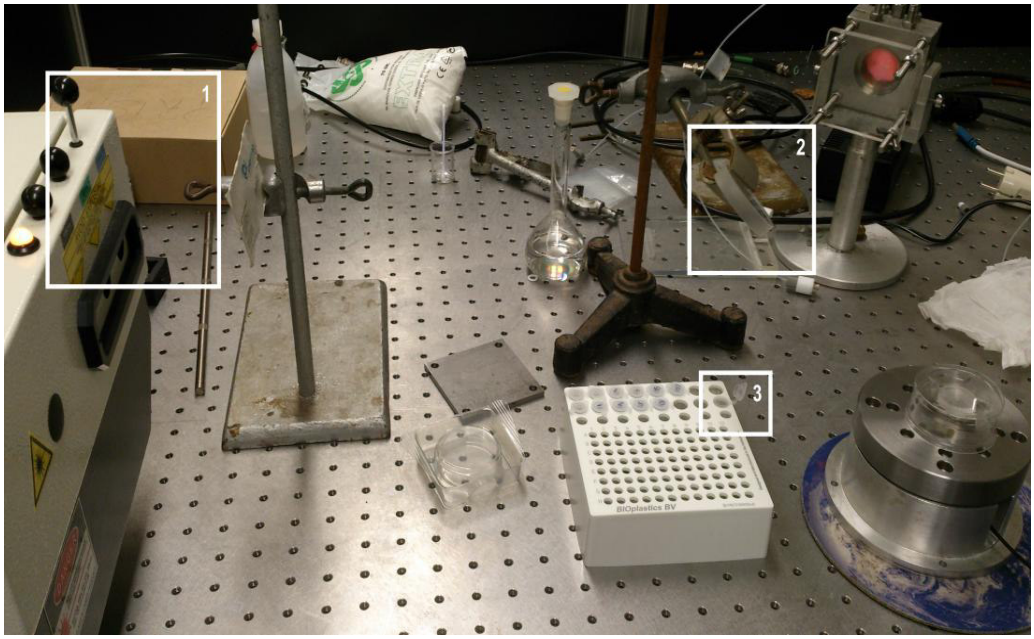

Figure 4. Arrangement set to irradiate the cells using a picosecond laser. The laser pulses leave the port (1), are reflected in the mirror (2), and reach the pellet of cell in the bottom of the tube (3). For the last part, it is important to take notice that the lid has to be open during the irradiation (plastic is not transparent to 266 nm wavelength), and that the surface of the pellet has to be completely covered by the area of the laser pulses.

Scheme 2. Schematic representation of the steps used to generate the CT26 whole-cell vaccines using PDT

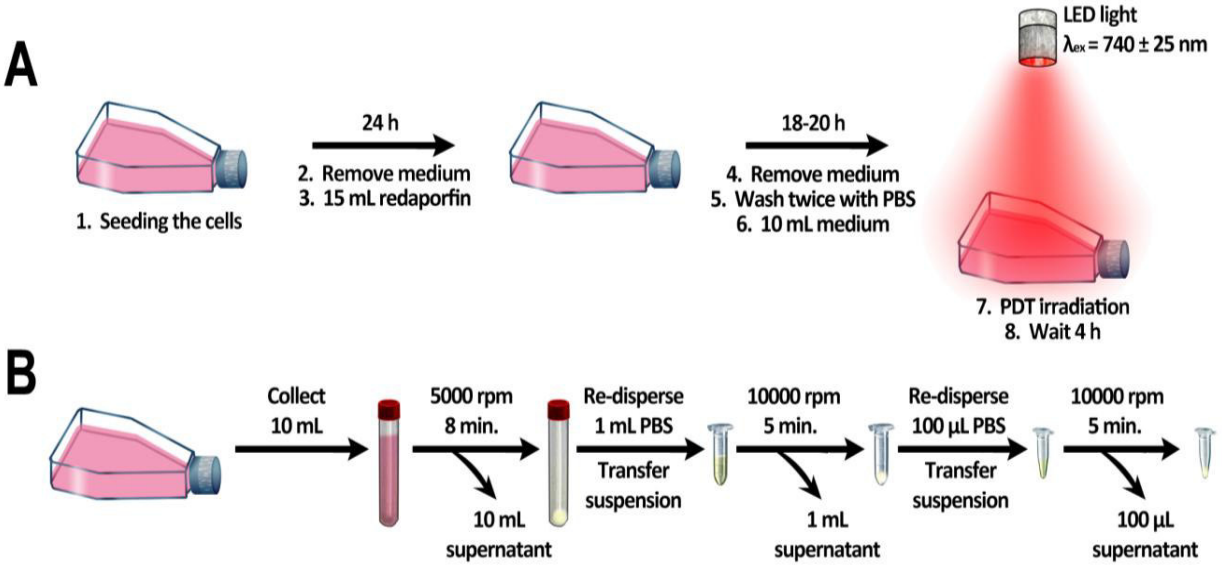

(A) *In vitro* PDT protocol. (B) Protocol to isolate the apoptotic cells after PDT and generate the vaccines.

Scheme 3. Schematic representation of the steps used to generate the CT26 whole-cell vaccines MTX

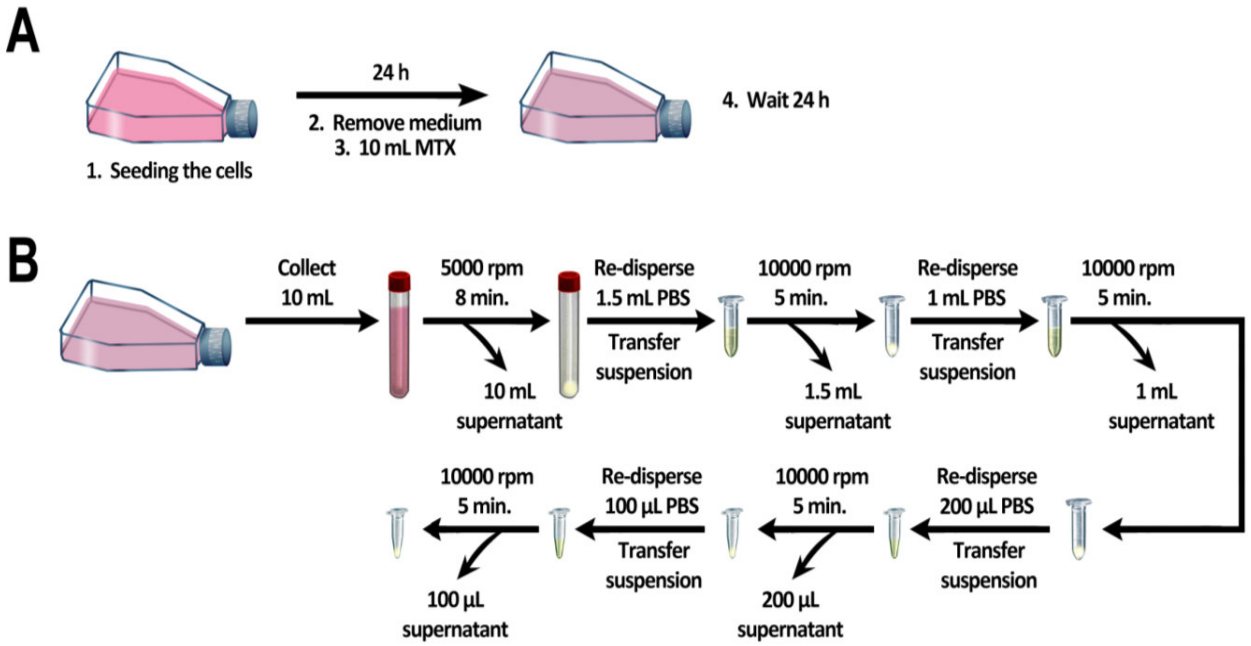

(A) *In vitro* MTX protocol. (B) Protocol to isolate the apoptotic cells after MTX incubation and generate the vaccines.

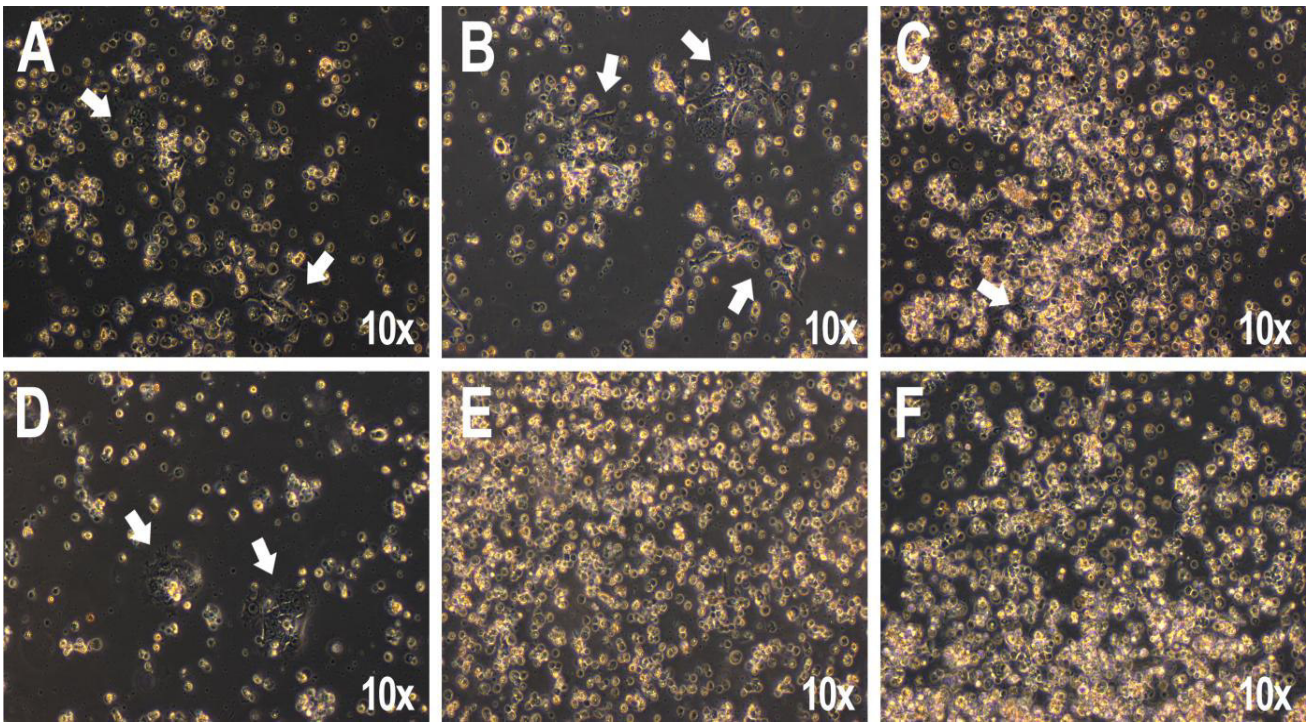

Figure 5. Viability of 300,000 4T1 cells, 48h after UV irradiation: (A) 0.78 J, (B) 1.56 J, (C, D) 3.90 J, (E) 7.80 J, and (F) 15.6 J. The arrows indicate live cells.

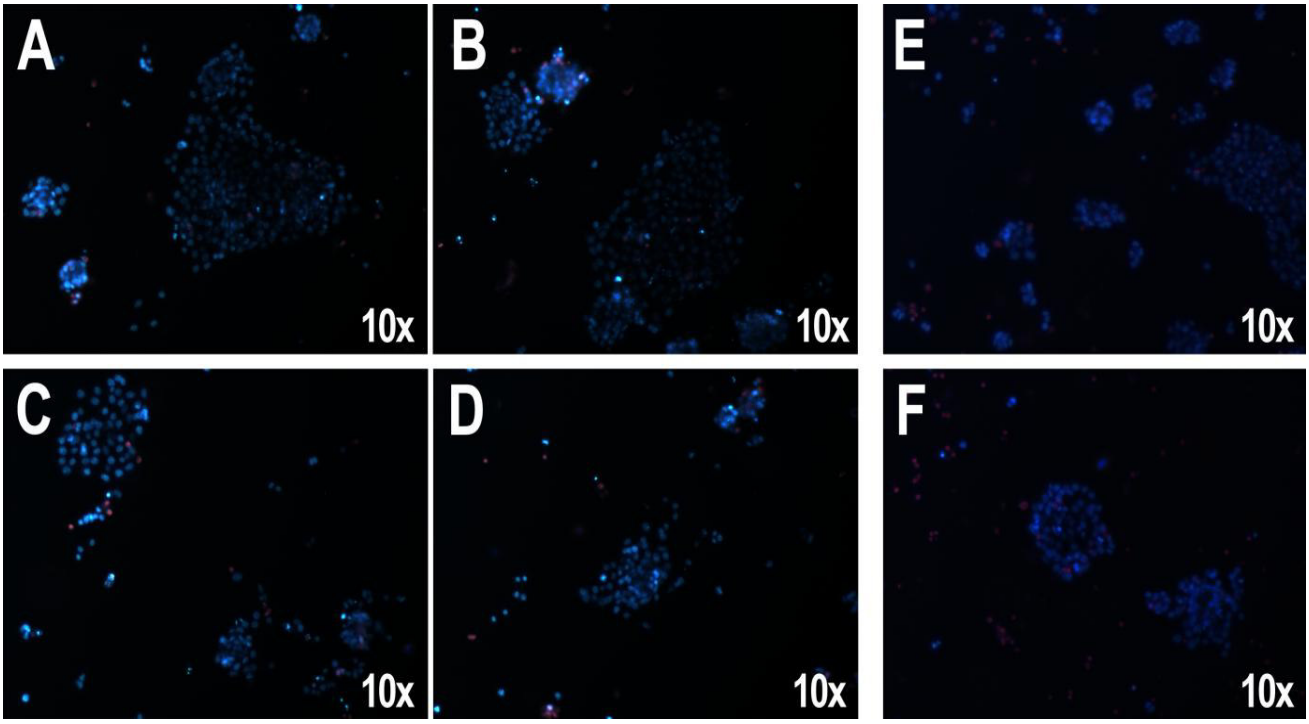

Figure 6. Viability of $3x10^6$ 4T1 cells with fluorescent assays, 24h after UV irradiation: (A) 12.0 J; (B) 18.0 J; (C) 27.0 J; and (D) 36.0 J. Viability of two different irradiation protocols for UV control group with fluorescent assays: (E) $3x10^6$ 4T1 cells were irradiated 18 J, re-dispersed in PBS, centrifuged at 3000 rpm for 5 min, and irradiated with more 18 J after discarding the supernatant; (F) two pellets of $1.5x10^6$ 4T1 cells were irradiated with 18.0 J of UV radiation. The fluorescent dyes are Hoechst in blue, and PI in red.

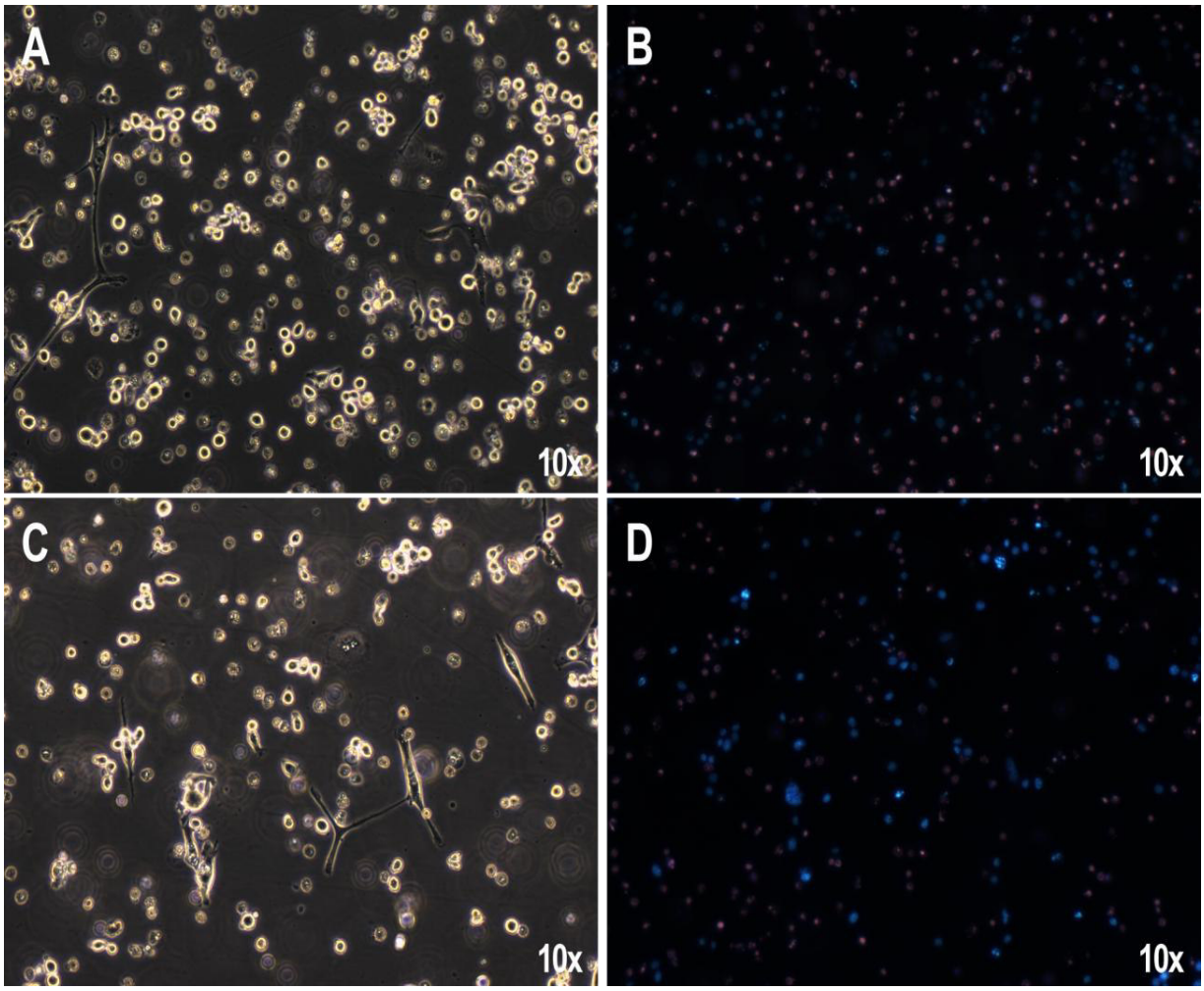

Figure 7. Viability of CT26 cells, 24h after PDT protocol. (A) Cells from the PDT_{500} group. (B) Stained cells from the PDT_{500} group. (C) Cells from the PDT_{300} group. (D) Stained cells from the PDT_{300} group. The fluorescent dyes are Hoechst in blue, and PI in red.

Tables

Table 1. *In vitro* PDT conditions for 4T1 cells to modulate type of cell death and ROS factor associated

[Redaporfin] (μM)	Light Dose (J/cm^2)	Type of cell death	ROS factor
0.21	0.05	Apoptosis ↓↓↓	0.0105
0.21	0.10	Apoptosis ↓↓↓	0.0211
0.21	0.15	Apoptosis ↓↓	0.0316
0.21	0.20	Apoptosis ↓↓	0.0421
0.21	0.25	Apoptosis ↓	0.0527
0.21	0.30	Apoptosis ↓	0.0632
0.42	0.25	Apoptosis	0.1054
0.42	0.30	Apoptosis	0.1264
0.63	0.25	Apoptosis	0.1581
1.26	0.15	Apoptosis	0.1897
0.63	0.30	Apoptosis	0.1897
0.63	0.35	Apoptosis; Necrosis ↓↓	0.2213
1.05	0.30	Necrosis; Apoptosis ↓↓	0.3161
1.26	0.30	Apoptosis ↓↓	0.3793
1.05	0.40	Necrosis	0.4215
1.26	0.40	Apoptosis ↓↓	0.5058
1.05	0.50	Necrosis	0.5269
1.05	0.52	Necrosis	0.5479
1.05	0.56	Necrosis	0.5901
1.26	0.50	Apoptosis; Necrosis ↓↓	0.6322
1.05	0.60	Necrosis	0.6322
2.11	0.60	Necrosis	1.2645
0.63	2.00	Necrosis	1.2645
2.11	0.70	Necrosis	1.4752
2.11	0.80	Necrosis	1.6860
1.26	2.00	Necrosis	2.5289
1.05	3.00	Necrosis	3.1612
1.26	3.00	Necrosis	3.7934
2.11	5.00	Necrosis	10.5372
2.11	6.00	Necrosis	12.6446
2.11	7.00	Necrosis	14.7521

The conditions underlined were the ones chosen for the PDT protocol.

Table 2. 4T1 whole-cell vaccine protocol: measurements and statistics on the evaluation of tumour growth in animals from the Control group (PBS)

Mouse no.	Day 14				Day 21			
	a (mm)	b (mm)	Vol (mm^3)	X_m	a (mm)	b (mm)	Vol (mm^3)	X_m
1	3.4	3.4	19.652	16.303	5.0	4.1	42.025	53.566
2	4.0	3.7	27.380	**SEM**	5.9	5.6	95.512	**SEM**
3	2.9	2.6	9.8020	2.597	5.8	4.1	48.749	8.107
4	3.2	3.1	15.376	**N**	5.1	4.6	53.958	**N**
5	3.1	2.8	12.152	6	5.0	4.3	46.225	6
6	3.2	2.9	13.456		4.3	4.2	37.926	

Mouse no.	Day 28				Day 33			
	a (mm)	b (mm)	Vol (mm^3)	X_m	a (mm)	b (mm)	Vol (mm^3)	X_m
1	7.0	6.7	157.115	164.229	8.1	7.8	246.402	313.345
2	8.0	6.8	184.960	**SEM**	9.3	8.8	360.096	**SEM**
3	9.4	6.7	210.983	12.099	10.0	8.9	396.050	30.365
4	6.8	6.6	148.104	**N**	8.3	7.7	246.054	**N**
5	6.8	6.1	126.514	6	8.1	7.8	246.402	6
6	7.7	6.4	157.696		9.3	9.1	385.067	

Where: *a* is the major axis of the tumour, *b* is the minor axis of the tumour, Vol is tumour volume (calculated using equation 4), X_m is the mean of tumour volumes, SEM, is the standard error of the mean, N is the number of animals at the timepoint.

Table 3. 4T1 whole-cell vaccine protocol: measurements and statistics on the evaluation of tumour growth in animals from the UV control group

Mouse no.	Day 14				Day 21			
	a (mm)	b (mm)	Vol (mm^3)	X_m	a (mm)	b (mm)	Vol (mm^3)	X_m
1	3.9	3.5	23.888	28.141	6.6	4.5	66.825	148.497
2	3.7	3.0	16.650	**SEM**	5.0	3.9	38.025	**SEM**
3	5.4	5.3	75.843	11.029	9.3	6.7	208.739	75.045
4	n/m	n/m	"0.000"	**N**	5.6	3.7	38.332	**N**
5	5.1	4.0	40.800	6	10.6	9.7	498.677	6
6	3.2	2.7	11.664		5.9	3.7	40.386	

Mouse no.	Day 28				Day 33			
	a (mm)	b (mm)	Vol (mm^3)	X_m	a (mm)	b (mm)	Vol (mm^3)	X_m
1	8.0	5.9	139.240	329.704	10.2	7.3	271.779	405.841
2	7.3	6.2	140.306	**SEM**	9.8	7.9	305.809	**SEM**
3	12.3	6.9	292.802	163.902	14.9	10.3	790.371	98.864
4	7.8	5.3	109.551	**N**	11.5	7.4	314.870	**N**
5	15.3	12.2	1138.626	6				5
6	12.2	7.9	157.696		11.1	7.9	346.376	

Where: *a* is the major axis of the tumour, *b* is the minor axis of the tumour, Vol is tumour volume (calculated using equation 4), X_m is the mean of tumour volumes, SEM, is the standard error of the mean, N is the number of animals at the timepoint. "n/m" means non-measurable (the tumour was palpable but could not be measured).

Table 4. 4T1 whole-cell vaccine protocol: measurements and statistics on the evaluation of tumour growth in animals from the Necrosis/UV group

Mouse no.	Day 14				Day 21			
	a (mm)	b (mm)	Vol (mm^3)	X_m	a (mm)	b (mm)	Vol (mm^3)	X_m
1	3.4	3.1	16.337	21.116	5.0	4.2	44.100	58.963
2	3.7	3.0	16.650	**SEM**	4.3	4.2	37.926	**SEM**
3	2.9	2.6	9.802	3.323	5.1	4.1	42.866	8.901
4	5.3	3.1	25.467	**N**	6.4	5.2	86.528	**N**
5	4.4	3.5	26.950	6	5.9	4.4	57.112	6
6	4.6	3.7	31.487		7.4	4.8	85.248	

Mouse no.	Day 28				Day 33			
	a (mm)	b (mm)	Vol (mm^3)	X_m	a (mm)	b (mm)	Vol (mm^3)	X_m
1	6.5	6.4	133.120	280.325	8.9	7.2	230.688	402.076
2	7.2	6.0	129.600	**SEM**	8.9	7.5	250.313	**SEM**
3	9.9	7.9	308.930	32.537	11.5	10.2	598.230	67.589
4	8.8	8.1	288.684	**N**	11.5	10.2	598.230	**N**
5	7.4	6.5	156.325	6	9.4	8.2	316.028	6
6	9.8	6.9	233.289		9.9	9.2	418.968	

Where: *a* is the major axis of the tumour, *b* is the minor axis of the tumour, Vol is tumour volume (calculated using equation 4), X_m is the mean of tumour volumes, SEM, is the standard error of the mean, N is the number of animals at the timepoint.

Table 5. 4T1 whole-cell vaccine protocol: measurements and statistics on the evaluation of tumour growth in animals from the Apoptosis/UV group

Mouse no.	Day 14				Day 21			
	a (mm)	b (mm)	Vol (mm^3)	X_m	a (mm)	b (mm)	Vol (mm^3)	X_m
1	n/m	n/m	"0.000"	10.595	6.6	4.5	66.825	86.990
2	n/m	n/m	"0.000"	**SEM**	5.0	3.9	38.025	**SEM**
3	5.3	2.7	19.319	5.114	9.3	6.7	208.739	31.569
4	3.3	3.0	14.850	**N**	5.6	3.7	38.332	**N**
5	5.4	3.3	29.403	6	10.6	9.7	498.677	6
6	0.0	0.0	0.000		5.9	3.7	40.386	

Mouse no.	Day 28				Day 33			
	a (mm)	b (mm)	Vol (mm^3)	X_m	a (mm)	b (mm)	Vol (mm^3)	X_m
1	8.0	5.9	139.240	239.446	10.2	7.3	271.779	375.276
2	7.3	6.2	140.306	**SEM**	9.8	7.9	305.809	**SEM**
3	12.3	6.9	292.802	40.409	14.9	10.3	790.371	72.310
4	7.8	5.3	109.551	**N**	11.5	7.4	314.870	**N**
5	15.3	12.2	1138.626	6				5
6	7.7	6.4	157.696		11.1	7.9	346.376	

Where: *a* is the major axis of the tumour, *b* is the minor axis of the tumour, Vol is tumour volume (calculated using equation 4), X_m is the mean of tumour volumes, SEM, is the standard error of the mean, N is the number of animals at the timepoint. "n/m" means non-measurable (the tumour was palpable but could not be measured).

Table 6. 4T1 whole-cell vaccine protocol: statistical analysis results using Student's t-test to compare significant statistical difference between the treatment groups and the control.

Day 14	Control	UV Control	Necrosis/UV	Apoptosis/UV
X_m	16.303	28.141	21.116	10.595
P (T ≤ t)		0.336	0.283	0.352
N	6	6	6	6

Day 21	Control	UV Control	Necrosis/UV	Apoptosis/UV
X_m	53.566	148.497	58.963	86.990
P (T ≤ t)		0.264	0.663	0.345
N	6	6	6	6

Day 28	Control	UV Control	Necrosis/UV	Apoptosis/UV
X_m	164.229	329.704	280.325	239.446
P (T ≤ t)		0.360	0.251	0.125
N	6	6	6	6

Day 33	Control	UV Control	Necrosis/UV	Apoptosis/UV
X_m	313.345	405.841	402.076	375.276
P (T ≤ t)		0.404	0.270	0.466
N	6	6	5	5

Where: X_m is the mean of tumour volumes, P (T ≤ t) is the probability of the test value T being equal/inferior to the critical value t, N is the number of animals at the timepoint.

Table 7. CT26 whole-cell vaccine protocol: measurements and statistics on the evaluation of tumour growth in animals from the Control group

Mouse no.	Day 14				Day 17			
	a (mm)	**b (mm)**	**Vol (mm^3)**	**X_m**	**a (mm)**	**b (mm)**	**Vol (mm^3)**	**X_m**
1	n/m	n/m	"0.000"	60.237	6.1	4.9	73.231	193.053
2	2.5	2.1	5.513	**SEM**	8.6	5.1	111.843	**SEM**
3	9	8	288.000	56.961	13.6	10.2	707.472	129.381
4	n/m	n/m	"0.000"	**N**	4.5	3.6	29.160	**N**
5 †				5				5
6	2.9	2.3	7.671		4.5	4.4	43.560	

Mouse no.	Day 21				Day 24			
	a (mm)	**b (mm)**	**Vol (mm^3)**	**X_m**	**a (mm)**	**b (mm)**	**Vol (mm^3)**	**X_m**
1	8.6	6.5	181.675	429.874	14.1	9.2	596.712	614.062
2	11.3	7.2	292.896	**SEM**	15.1	10.6	848.318	**SEM**
3	14.8	13.4	1328.744	225.954				84.629
4	11.5	5.8	38.786	**N**	15.3	8.6	565.794	**N**
5 †				5				4
6	6.8	6.7	81.648		10.3	9.3	445.424	

Mouse no.	Day 28				Day 31			
	a (mm)	**b (mm)**	**Vol (mm^3)**	**X_m**	**a (mm)**	**b (mm)**	**Vol (mm^3)**	**X_m**
1	16.0	11.9	1132.880	1054.350				1584.798
2				**SEM**				**SEM**
3				78.530				
4				**N**				**N**
5 †				2				1
6	12.9	12.3	1584.798		15.5	14.3	1584.798	

Where: *a* is the major axis of the tumour, *b* is the minor axis of the tumour, Vol is tumour volume (calculated using equation 4), X_m is the mean of tumour volumes, SEM, is the standard error of the mean, N is the number of animals at the timepoint. "n/m" means non-measurable (the tumour was palpable but could not be measured).

† This animal was not inoculated with the tumour challenge

Table 8. CT26 whole-cell vaccine protocol: measurements and statistics on the evaluation of tumour growth in animals from the MTX group

Mouse no.	Day 14				Day 17			
	a (mm)	b (mm)	Vol (mm^3)	X_m	a (mm)	b (mm)	Vol (mm^3)	X_m
1	2.3	1.9	4.152	8.275	5.6	3.9	42.588	83.302
2	0.0	0.0	0.000	**SEM**	5.2	3.7	35.594	**SEM**
3	0.0	0.0	0.000	7.475	0.0	0.0	0.000	43.628
4	4.7	4.4	45.496	**N**	6.8	6.7	152.626	**N**
5	0.0	0.0	0.000	6	8.2	8.1	269.001	6
6	0.0	0.0	0.000		0.0	0.0	0.000	

Mouse no.	Day 21				Day 24			
	a (mm)	b (mm)	Vol (mm^3)	X_m	a (mm)	b (mm)	Vol (mm^3)	X_m
1	6.7	4.5	67.838	245.668	9.7	7.9	302.689	442.602
2	6.3	4.4	60.984	**SEM**	9.8	5.1	127.449	**SEM**
3	3.9	3.0	17.550	118.199	6.0	4.3	55.470	202.244
4	11.6	9.3	501.642	**N**	15.0	9.6	691.200	**N**
5	12.0	10.9	712.860	6	14.7	13.5	1339.538	6
6	6.5	5.9	113.133		6.8	6.4	139.264	

Mouse no.	Day 28				Day 31			
	a (mm)	b (mm)	Vol (mm^3)	X_m	a (mm)	b (mm)	Vol (mm^3)	X_m
1	10.7	9.0	433.350	421.747	15.7	9.2	664.424	641.053
2	11.6	6.3	230.202	**SEM**	15.3	9.4	675.954	**SEM**
3	8.6	5.7	139.707	165.780	10.6	6.8	245.072	150.724
4				**N**				**N**
5				4				4
6	13.6	11.4	883.728		14.3	11.7	978.764	

Where: *a* is the major axis of the tumour, *b* is the minor axis of the tumour, Vol is tumour volume (calculated using equation 4), X_m is the mean of tumour volumes, SEM, is the standard error of the mean, N is the number of animals at the timepoint.

Table 9 CT26 whole-cell vaccine protocol: measurements and statistics on the evaluation of tumour growth in animals from the PDT_{500} group

Mouse no.	Day 14				Day 17			
	a (mm)	**b (mm)**	**Vol (mm^3)**	**X_m**	**a (mm)**	**b (mm)**	**Vol (mm^3)**	**X_m**
1	0.0	0.0	0.000	54.515	0.0	0.0	0.000	95.168
2	0.0	0.0	0.000	**SEM**	n/m	n/m	"0.000"	**SEM**
3	0.0	0.0	0.000	43.832	2.5	2.3	6.613	68.541
4	8.6	7.9	268.363	**N**	11.0	8.7	416.295	**N**
5	5.8	4.5	58.725	6	6.8	6.6	148.104	6
6	0.0	0.0	0.000		0.0	0.0	0.000	

Mouse no.	Day 21				Day 24			
	a (mm)	**b (mm)**	**Vol (mm^3)**	**X_m**	**a (mm)**	**b (mm)**	**Vol (mm^3)**	**X_m**
1	0.0	0.0	0.000	229.816	0.0	0.0	0.000	336.079
2	4.1	2.9	17.241	**SEM**	5.8	4.1	48.749	**SEM**
3	5.7	4.9	68.429	138.737	10.4	7.2	269.568	161.814
4	16.3	10.5	898.538	**N**				**N**
5	8.4	7.6	242.592	6	13.2	11.6	888.096	5
6	7.2	6.5	152.100		11.2	9.2	473.984	

Mouse no.	Day 28				Day 31			
	a (mm)	**b (mm)**	**Vol (mm^3)**	**X_m**	**a (mm)**	**b (mm)**	**Vol (mm^3)**	**X_m**
1	0.0	0.0	0.000	670.4923	0.0	0.0	0.000	324.750
2	7.7	5.3	108.147	**SEM**	8.8	6.0	158.400	**SEM**
3	12.8	9.6	589.824	295.067	14.8	10.5	815.850	249.771
4				**N**				**N**
5	16.6	13.7	1557.827	5				4
6	16.3	11.6	1096.664					

Where: *a* is the major axis of the tumour, *b* is the minor axis of the tumour, Vol is tumour volume (calculated using equation 4), X_m is the mean of tumour volumes, SEM, is the standard error of the mean, N is the number of animals at the timepoint. "n/m" means non-measurable (the tumour was palpable but could not be measured).

Table 10. CT26 whole-cell vaccine protocol: measurements and statistics on the evaluation of tumour growth in animals from the PDT_{300} group

Mouse no.	Day 14				Day 17			
	a (mm)	**b (mm)**	**Vol (mm^3)**	**X_m**	**a (mm)**	**b (mm)**	**Vol (mm^3)**	**X_m**
1	5.0	4.0	40.000	11.703	6.5	4.9	78.033	93.819
2	0.0	0.0	0.000	**SEM**	5.4	5.0	67.500	**SEM**
3	0.0	0.0	0.000	7.931	8.2	6.5	173.225	24.592
4 †	~~0.0~~	~~0.0~~	~~0.000~~	**N**	~~n/m~~	~~n/m~~	~~"0.000"~~	**N**
5	0.0	0.0	0.000	5	4.1	3.8	29.602	5
6	3.4	3.3	18.513		7.7	5.6	120.736	

Mouse no.	Day 21				Day 24			
	a (mm)	**b (mm)**	**Vol (mm^3)**	**X_m**	**a (mm)**	**b (mm)**	**Vol (mm^3)**	**X_m**
1	10.3	8.1	337.892	411.285	11.8	11.4	766.764	694.250
2	11.7	6.9	278.519	**SEM**	14.8	10.5	815.850	**SEM**
3	13.5	11.2	846.720	138.969	16.3	12.8	1335.296	200.258
4 †	~~6.4~~	~~4.7~~	~~70.688~~	**N**	~~7.5~~	~~5.6~~	~~117.600~~	**N**
5	6.3	5.1	81.932	5	9.5	6.0	171.000	5
6	8.2	5.7	133.209		11.1	8.3	382.340	

Mouse no.	Day 28				Day 31			
	a (mm)	**b (mm)**	**Vol (mm^3)**	**X_m**	**a (mm)**	**b (mm)**	**Vol (mm^3)**	**X_m**
1	15.3	12.9	1273.037	892.447				786.662
2				**SEM**				**SEM**
3				229.387				249.675
4 †	~~9.2~~	~~8.7~~	~~348.174~~	**N**				**N**
5	11.6	9.1	480.298	3	11.9	9.5	536.988	2
6	13.5	11.7	924.008		13.7	12.3	1036.337	

Where: *a* is the major axis of the tumour, *b* is the minor axis of the tumour, Vol is tumour volume (calculated using equation 4), X_m is the mean of tumour volumes, SEM, is the standard error of the mean, N is the number of animals at the timepoint. "n/m" means non-measurable (the tumour was palpable but could not be measured).

† This animal developed a secondary tumour from the vaccine that reached the 1.5cm before the challenge tumour had reached any of the endpoints. It was not accounted for the statistical analysis.

Table 11. CT26 whole-cell vaccine protocol: statistical analysis results using Student's t-test to compare significant statistical difference between the treatment groups and the control.

Day 14	Control	MTX	PDT_{500}	PDT_{300}
X_m	60.237	8.275	54.515	11.703
P (T ≤ t)		0.424	0.948	0.446
N	5	6	6	5

Day 17	Control	MTX	PDT_{500}	PDT_{300}
X_m	193.053	83.3015	95.169	93.8191
P (T ≤ t)		0.458	0.529	0.493
N	5	6	6	5

Day 21	Control	MTX	PDT_{500}	PDT_{300}
X_m	429.874	245.668	229.816	411.285
P (T ≤ t)		0.497	0.475	0.946
N	225.954	6	6	5

Day 24	Control	MTX	PDT_{500}	PDT_{300}
X_m	614.062	442.602	336.079	375.276
P (T ≤ t)		0.460	0.179	0.727
N	4	6	5	5

Day 28	Control	MTX	PDT_{500}	PDT_{300}
X_m	1054.35	421.747	670.492	892.447
P (T ≤ t)		0.026 †	0.277	0.573
N	2	4	5	3

Day 31	Control	MTX	PDT_{500}	PDT_{300}
X_m	1584.798	641.053	3214.750	786.662
P (T ≤ t)				
N	1	4	3	2

Where: X_m is the mean of tumour volumes, P (T ≤ t) is the probability of the test value T being equal/inferior to the critical value t, N is the number of animals at the timepoint.

† Significant statistical difference ($P < 0.05$)